in a single perinuclear spot. The distance between PfSET10 and *var2csa* and PFL0020w loci was measured to achieve unbiased results (Figures 2A and S2B) and found to be significantly smaller in parasites where the *var* gene was active ("on") (Kolmogorov-Smirnov test: "on" distribution is shifted to smaller distances compared to "off", with p value = 0.9952).

To define the position of silenced *var* gene clusters with respect to PfSET10 expression, we used antibodies to PfHP1, a protein localizing with chromosome end clusters and histone mark H3K9me3, which are both associated with silenced *var* gene clusters (Flueck et al., 2009). PfHP1 and the histone mark H3K9me3 showed no overlap with PfSET10 expression (Figures 2C and 2D). The association of PfHP1 with the silent *var* gene was confirmed by IFA-FISH on CSA selected (*var2csa* "on") and nonselected (*var2csa* "off") 3D7HP1-GFP (Figure 2B). The distance between PfHP1 and the *var2csa* locus was measured to achieve unbiased results (Figures 2B and S2B) and was significantly smaller in parasites where the *var* gene was silent ("off"). Also the distance to the second nearest PfHP1 demarcated telomere cluster was significantly smaller (Figures 2B and S2B). Taken together, these results show that PfSET10 localizes to a perinuclear compartment of the nucleus shared by the active *var* gene.

PfSET10 Is a Histone Lysine 4 Methyltransferase

PfSET10 shows homology to histone lysine methyltransferases (HKMT) of the SET domain-containing protein family (Figure S3A) (Cui et al., 2008; Dillon et al., 2005). The SET domain distinguishes substrates and performs the catalytic activity (Trievel et al., 2002). Site-specific histone methylation serves either transcriptional gene activation or silencing and is dynamically regulated by interplay of HKMTs and histone lysine demethylases. PfSET10 is conserved within the Apicomplexan lineage; however, multiple sequence alignment based on structural information of PfSET10 revealed no similarity of the PfSET10 SET domain to any other known HKMT SET domain (Figure S3A). As well as a SET domain, PfSET10 contains a plant-like homeodomain (PHD) (Figure S3B), a structural motif involved in recognition of methylated or unmodified histone H3 (Mellor, 2006). The PHD finger domain displays highest similarity to uncharacterized PHD finger domains of *Arabidopsis thaliana* and *Toxoplasma gondii* (Figure S3B). Interestingly, PfSET10 PHD finger domain shares a number of amino acid residues with PHD finger domains that preferentially bind nonmethylated histone H3 (Figure S3B) (Lan et al., 2007; Org et al., 2008).

To determine the potential histone-binding properties of the PfSET10 PHD finger domain, we expressed and purified the PfSET10 SET/PHD (SET/PHD) domains including a control, which lacked the PHD finger (SET10/ΔPHD), using cell-free wheat germ expression (Figures 3A and S3C) (Tsuboi et al., 2010). In Far Western analysis using *P. falciparum* histone extracts as well as a histone peptide-binding assay, recombinant SET/PHD domain (Figures 3B and 3C) preferentially binds to histone H3 with highest affinity for the nonmethylated and monomethylated lysine 4 residue, which decreased upon di- and trimethylation or methylation of H3K9 (Figures 3B and 3C). Since the SET domain alone does not exert similar binding activity, the PHD finger was sufficient for H3 tail binding. PfSET10 binding to histone H2A cannot be excluded since histone H3 and H2A comigrate in the gel (Figure 3B) and PfSET10 colocalizes in IFA with histone H2A, but not H2.AZ (Figure 3D).

To determine if PfSET10 is a HKMT, we tested methyltransferase activity of the recombinant SET/PHD protein and a mutant form of the SET domain (ΔSET/PHD) (Figure S3C) using histone peptides, nucleosomes, or recombinant histones as substrates. The recombinant SET/PHD protein showed no detectable methyltransferase activity (data not shown). This observation indicated that PfSET10 may only be active as full-length protein or when present in a multiprotein complex (Briggs et al., 2001; Krogan et al., 2002; Nagy et al., 2002; Roguev et al., 2001). Therefore PfSET10 was immunoprecipitated from the 3D7SET10-HA parasites. Using recombinant histones as substrates, we were able to detect specific histone H3 methylation (Figure 3E) at an approximately 5-fold higher level compared to control (HA precipitate from 3D7), while methyltransferase activity toward histone H4 was considerably lower. Methylated lysines were detected with specific antibodies, and this indicated that incubation with PfSET10 increased di- and trimethylation of H3K4 (Figure 3E). PfSET10 also colocalized with the H3K4me1, me2, and me3 marks in the perinuclear region, which is also marked by H3K9ac (Figure 3F). While we cannot eliminate the possibility that enzymatic activity resides in another protein in the PfSET10 complex, sequence homology to the HKMT of the SET domain-containing protein family strongly indicate that PfSET10 preferentially targets and methylates lysine 4 (K4) on H3.

PfSET10 Interacts with PfActin-1

To identify proteins that are associated with PfSET10 in the *var* gene expression site, we performed immunoprecipitations on 3D7SET10-HA and 3D7 (negative control) using anti-HA antibody and identified associated proteins by LC-MS/MS (Figures 4, S4A, S4B, and Table S2). While a number of nuclear proteins were identified, including histone H2A (Figures 3B, 3D, and 4A), the presence of PfActin-1 was of interest, as it can be involved in gene transcription control through chromatin remodeling and directing movements of gene loci toward a target region (Visa and Percipalle, 2010). While PfActin-1 was distributed in speckles throughout the nucleus (Figure S4C), it showed colocalization with PfSET10 during late ring/early trophozoite stages (Figures 4B and S4C). The association of PfSET10 and PfActin-1 was confirmed by immunoprecipitation and immunoblot analysis (Figure 4B). These results indicate that PfActin-1 is a component of the *var* gene expression site.

C-Terminal GFP Tagging Compromises PfSET10 Function

To determine PfSET10 function in vivo and its potential involvement in *var* gene regulation, we attempted to disrupt the gene via homologous recombination (Figure S5A) and in parallel via a recently established conditional knockout system by which the expression of candidate proteins can be controlled (Figures S5B and S5C) (Armstrong and Goldberg, 2007). Interestingly, we were not able to disrupt the *pfset10* locus or destabilize PfSET10 expression. This indicated that PfSET10 was refractory to deletion, suggesting it is essential for parasite survival.

Initially, the endogenous *Pf*SET10 protein had been fused to GFP for live cell imaging analysis (Volz et al., 2010); however,

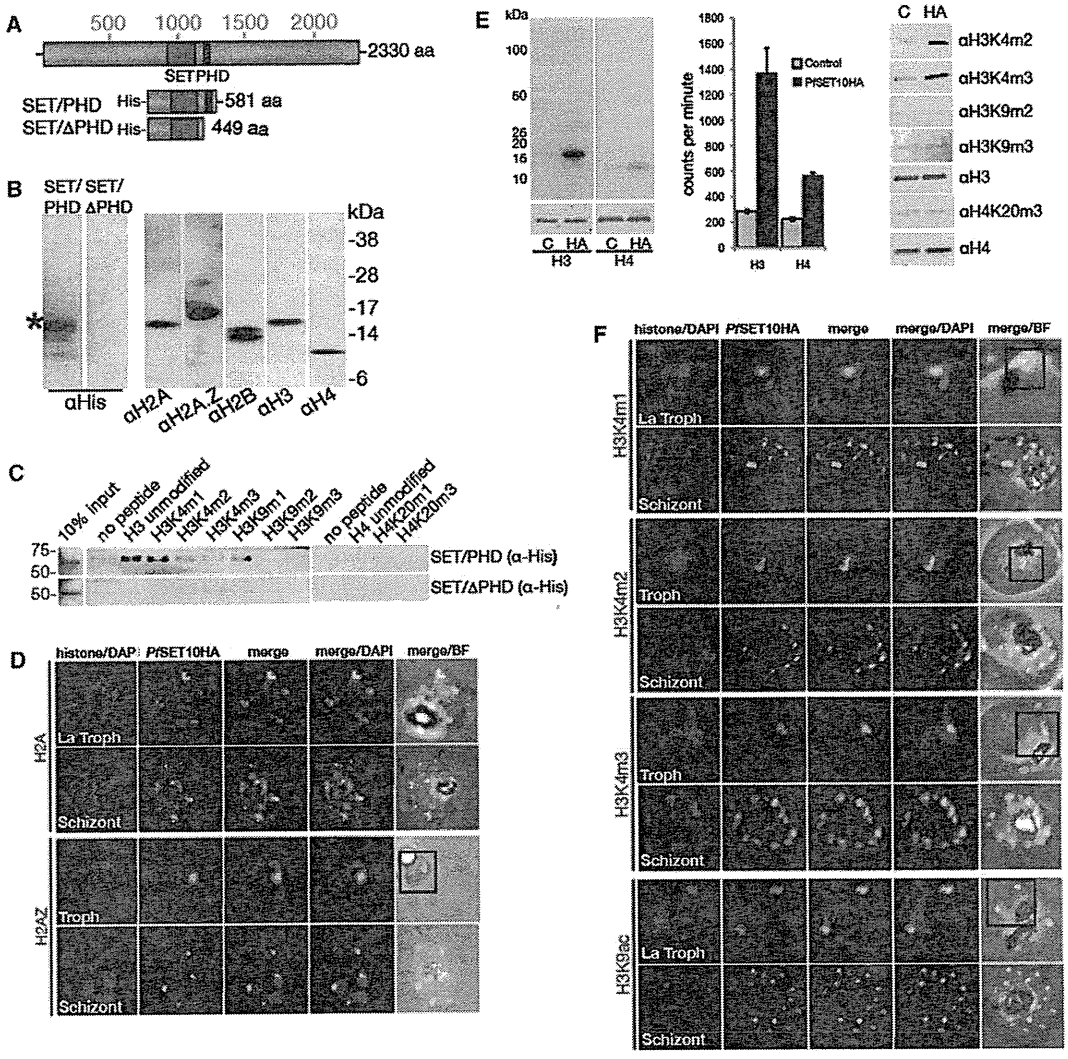

Figure 3. PfSET10 Is a Histone 3 Lysine 4 Methyltransferase

(A) Structure of PfSET10 showing the SET and PHD finger domains. Below are SET/PHD and SET/ΔPHD domains expressed as recombinant proteins with His tags.

(B) Far Western blot of *P. falciparum* histone extract using SET/PHD recombinant protein to show binding to histone H3 or potentially H2A (detected by anti-His antibodies; first panel). Subsequent panels are immunoblots of input material detecting H2A, H2A.Z, H2B, H3, and H4 with specific antibodies.

(C) Binding of SET/PHD to histone H3 and modified histone 3 peptides. SET/ΔPHD is shown as a negative control.

(D) Colocalization of histone H2A (two upper panels), but not H2A.Z (two lower panels) with PfSET10. The histones (red) were detected using specific antibodies and colocalized with PfSET10 (green) using anti-HA antibodies. Nucleus position is shown by DAPI.

(E) Immunoprecipitated PfSET10-HA has H3 methyltransferase activity in vitro. Recombinant human H3 and H4 were tested as substrates using radiolabeled SAM as methyl donor. The upper panels show the fluorograph in which H3 is preferentially labeled compared to H4. "C" is the immunoprecipitation from control parasites 3D7 while "HA" was from 3D7SET10HA. The bottom panels show a Coomassie-stained gel as a loading control. Data are represented as mean ± SEM of eight and six independent experiments of the activation assay using H3 and H4 as substrates, respectively. Reactions were also measured in a scintillation counter (middle panel). Methylated histone was detected using specific antibodies for the indicated histone marks (right panel).

(F) Colocalization of histone H3 marks with PfSET10. Shown are from top to bottom: H3K4m1, H3K4m2, H3K4m3, and H3K9ac. The histone marks (red) were detected using specific antibodies and colocalized with *Pf*SET10-HA (green) using anti-HA antibodies. Nucleus position is shown by DAPI staining. See also Figure S3.

we observed in at least two 3D7SET10-GFP parasite clones a growth phenotype compared to 3D7 and 3D7SET10-HA, suggesting the GFP tag had affected its function (Figure S5D). Since PfSET10 appeared refractory to genetic knockout or knockdown approaches, the phenotypic analysis of 3D7SET10-GFP parasites presented an opportunity to shed light on PfSET10 function. Localization studies implied that PfSET10 had a role in *var* gene regulation, so in order to determine potentially altered *var*

A 3D7/*Pf*SET10HA pulldown

PlasmoDB Accession[a]	Annotation	Coverage (%)	MW kDa	Unique Peptides
PF10_0068	RNA binding protein, putative	17.1	29.5	7
PFL1170w	Polyadenylate-binding protein, putative	4	97.2	5
PF10_0325	haloacid dehalogenase-like hydrolase, putative	10.8	32.8	4
MAL13P1.257.	Putative uncharacterized protein	28	18.7	4
PF13_0328	Proliferating cell nuclear antigen	12.4	30.6	4
PFF0940c	Cell division cycle protein 48 homologue, putative	7	92.4	4
PFL2215w	Actin-1	16	41.9	3
PF14_0655	RNA helicase-1	5.78	45.3	2
PF10_0063	DNA/RNA-binding (Alba protein), putative	22	119.8	2
PF11_0062	Histone H2B	21	13.1	2
PFL2060c	RabGDI protein	6.54	52.3	2
PFE1050w	Adenosylhomocysteinase	5.1	53.8	2
PFF0860c	Histone H2A	22	14.1	2

[a]Accession numbers (www.plasmodb.org) of nuclear proteins exclusively detected in the HA-bound fraction.

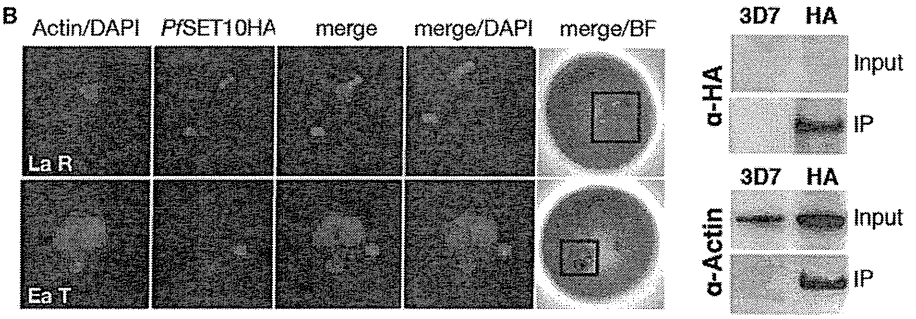

Figure 4. Identification of Proteins that Localize to the Active *var* Gene Expression Site

(A) Shown are proteins uniquely identified in the 3D7SET10-HA pull-down along with the number of unique peptides obtained and the percent of coverage. The PlasmoDB accession numbers of the genes identified are shown along with their functional annotation.

(B) IFA of PfSET10 (green) and PfActin-1 (red) with the nucleus (blue) stained with DAPI. First row, La R, late ring, second row, Ea T, early trophozoite. The right panels show immunoprecipitation of 3D7SET10-HA with anti-HA antibodies and detection of PfSET10-HA with anti-HA antibodies (left) and detection of PfActin-1 with PfActin-1 antibodies (right). See also Figure S4.

gene expression, 3D7SET10-GFP, 3D7, and 3D7SET10-HA parasites were selected for adherence to CSA to obtain those expressing *var2csa*. No changes in transcription of *var* genes other than *var2csa* was observed, indicating mutually exclusive expression in 3D7SET10-GFP remained intact (Figure 5A). However, we consistently observed an increased level of *var2csa* transcripts in 3D7SET10-GFP compared to 3D7 and 3D7SET10-HA (Figure 5A and data not shown). Increased *var2csa* transcription was further confirmed through the intraerythrocytic life cycle in 3D7SET10-GFP (Figure 5B). At ring stage (6–18 hr post invasion [p.i.]), we observed increased *var2csa* transcript in 3D7SET10-GFP, confirming the previous results. Strikingly, higher *var2csa* transcript levels were also observed at later stages (32–48 hr p.i.) in 3D7SET10-GFP parasites, while in 3D7 *var2csa* transcription was maintained in the typically quiescent poised state (Figure 5B).

The *var2csa* gene transcription that we have observed in late stages of 3D7SET10-GFP parasites suggests that chromatin around the gene must be accessible to the transcription machinery, similarly to that observed during ring stage at the active *var* locus. We performed chromatin-immunoprecipitation (ChIP) to determine the distribution of histone marks H3K4me2, H3K4me3, and H3K9ac, which are known marks for gene activation (Cui and Miao, 2010). In our control (3D7 parental parasites), which had been selected for *var2csa* expression, the level of these histone marks in the promoter region of the *var2CSA* gene was comparable to that observed for a euchromatic gene (*gbp130*) and higher than that of a silent *var* gene (PFL1960w) in ring and schizont stage parasites, respectively (Figure S6A). Moreover, H3K4me2 and me3 in the promoter of *var2csa* were enriched in 3D7SET10-GFP compared to the control (Figures 5C and S6B), with H3K9ac levels similar in both lines (Figure 5D). Therefore, the methylation levels of H3K4 of the poised *var* promoter are perturbed in 3D7/PfSET10GFP parasites, and this may account for the increased *var* gene expression pattern.

DISCUSSION

In *P. falciparum*, the nucleus is compartmentalized into heterochromatic and euchromatic regions, which distribution dynamically changes throughout the intraerythrocytic life cycle (Weiner et al., 2011). An intriguing feature in the *P. falciparum* nucleus is the presence of a zone of relaxed euchromatin within the nuclear

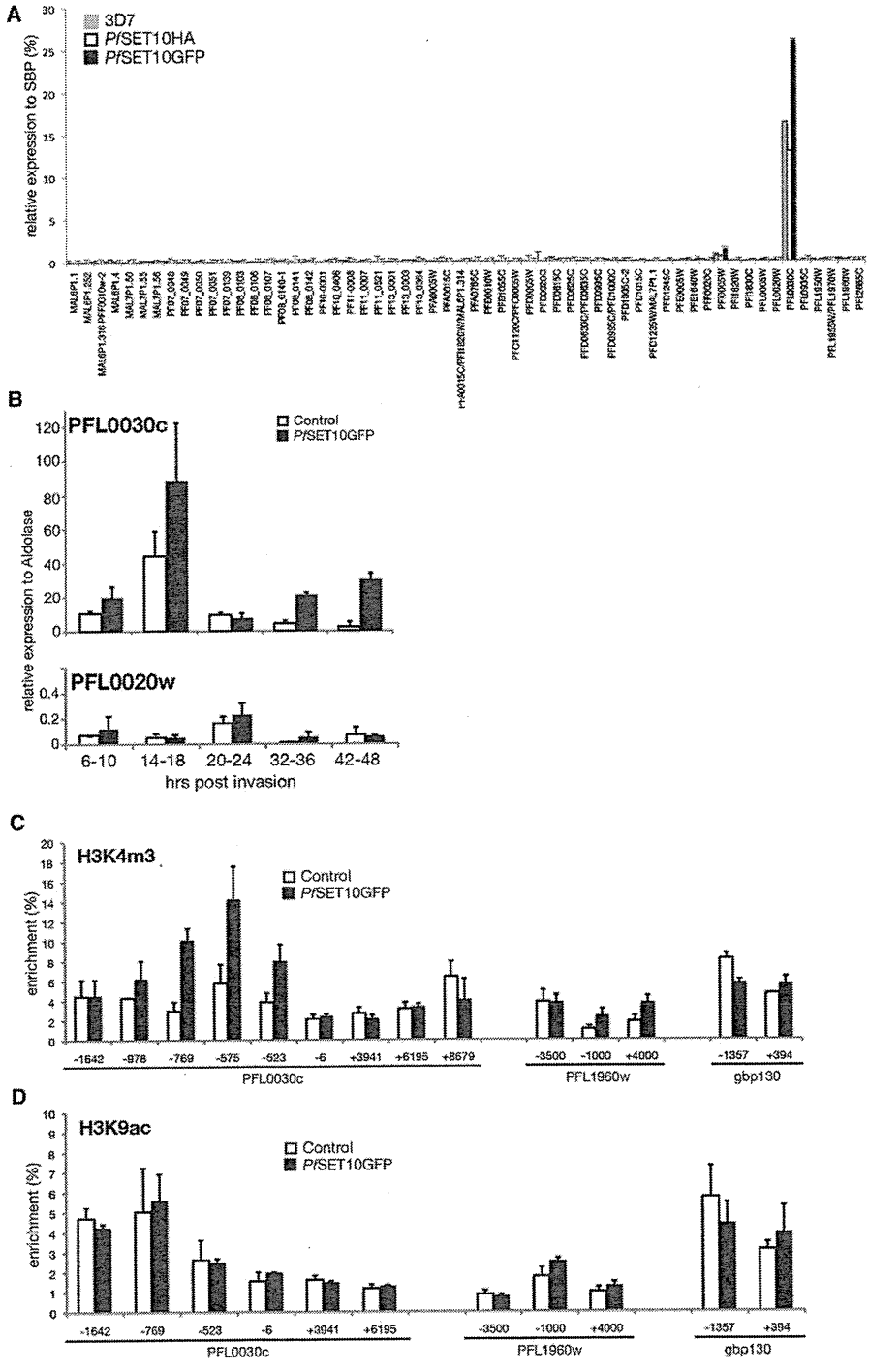

Figure 5. *Var2csa* Gene (PFL0030c) Is Dysregulated in 3D7SET10-GFP

(A) Quantitation of *var* gene transcripts for *var* in 3D7-CS, 3D7SET10-HA/CS, and 3D7SET10-GFP/CS parasites. Data are represented as mean ± SEM of two independent experiments.

(B) Quantitation of *var2csa* (PFL0030c) transcripts through the 48 hr cycle of 3D7-CS (control) versus 3D7SET10-GFP/CS compared to a silent *var* gene (PFL0020w). Data are represented as mean ± SEM of three independent experiments.

(C and D) (C) ChIP detecting the H3K4me3 mark in the *var2csa* (PFL0030c) gene compared to a silent *var* gene (PFL1960w) and *gbp130* gene as control. (D) ChIP detecting the H3K9ac mark as for (C). 3D7-CS served as wild-type control. Primer positions along the loci are indicated in relation to the start codon (ATG). See also Figures S5 and S6. Data in (C)are represented as mean ± SEM of two independent experiments and in (D) of three independent experiments.

periphery (Ralph et al., 2005). It has been speculated that this site may be specifically associated with transcription of the selected *var* gene from the 60 members of this multicopy virulence gene family (Duraisingh et al., 2005; Ralph et al., 2005; Voss et al., 2006). To date, this "expression site" was ill-defined and the molecular details of the mechanisms responsible for *var* gene translocation, activation, and poising remain almost completely unknown. In this study we have identified a protein, which we called PfSET10, that exclusively resides in this perinuclear expression site within an apparent euchromatic region. In contrast, we also confirmed that an inactive *var* gene was located within a chromosome end cluster marked by the presence of PfHP1 at the nuclear periphery. PfHP1 is involved in virulence gene silencing by maintaining a heterochromatic environment and establishing boundaries through its binding to histone mark H3K9me3 (Flueck et al., 2009). The active or poised *var2csa* gene did not colocalize with PfHP1 or the histone mark H3K9me3.

It is known from studies in eukaryotes, that transcriptionally active genes associate with so-called transcription factories (Osborne et al., 2004), which contain components of the transcription machinery such as RNA polymerase (Brown et al., 1999; Brown et al., 1997; Schübeler et al., 2000; Wang et al., 2004). Although human derived HeLa cells contain thousands of such transcription factories, numbers are restricted and several genes are translocated to the same site for transcription (Jackson et al., 1993). It is intriguing to speculate that the *var* gene transcription site, in which PfSET10 resides, might represent such a transcription factory to which *var* genes are translocated for activation.

As for *var* genes, members of the *rifin*, *stevor*, and *Pfmc-2TM* multigene families of *P. falciparum* undergo switched expression, indicating a potential role in antigenic variation (Kyes et al., 1999; Lavazec et al., 2007; Niang et al., 2009). Interestingly, it has recently been demonstrated, that a transcriptionally active episomal *rifin* promoter colocalizes with an active *var* promoter (Howitt et al., 2009). This indicates that members of the *rifin* multigene family may also translocate to this subnuclear expression site similar to the active *var*, and that possibly the expression site marked by PfSET10 is exclusively required for the transcription of virulence genes. At this stage, large-scale investigations into *P.falciparum* nuclear architecture, gene regulation, and movement are needed to clarify which set of genes translocate to the *var* gene/ PfSET10 transcription site for activation.

Interestingly, we identified PfActin-1 as a potential PfSET10-interacting protein. Nuclear actin can be part of the chromatin remodeling complex, involved in long-range chromatin organization and associated with the transcription machinery (Visa and Percipalle, 2010) or alternatively, together with myosin, may provide a molecular motor that steers gene loci toward the transcription site (Chuang et al., 2006; Dundr et al., 2007).

We have shown that PfSET10 has methyltransferase activity toward histone H3 lysine 4. In *P. falciparum*, three other SET-domain proteins have been predicted to have H3K4 methyltransferase activity, PfSET1 (PFF1440w), PfSET4 (PFI0485c), and PfSET6 (PF13_0293) (Cui et al., 2008). Localization studies in *P. falciparum* revealed that PfSET4 was present throughout the nucleus, while PfSET6 appeared to localize to the nucleolus (Volz et al., 2010). This observation suggests that *P. falciparum* H3K4 methylation may be performed in specific nuclear subcompartments by different HKMTs. Interestingly, in *Saccharomyces cerevisiae*, SET1 is the only enzyme responsible for H3K4 methylation (Briggs et al., 2001; Roguev et al., 2001), while in mammals at least ten known or predicted H3K4 methyltransferases exist. Deletion and phenotype analysis revealed that methyltransferases of the MLL family are not redundant in function; in contrast, they are specialized and differentially expressed being recruited to different gene loci (Glaser et al., 2006; Lee et al., 2006; Yu et al., 1995).

In various organisms, di- and trimethylation of the H3K4 site are enriched at actively transcribed genes (Bernstein et al., 2002; Santos-Rosa et al., 2002). In *S. cerevisiae*, poised genes are largely dimethylated at H3K4 (Ng et al., 2003; Pokholok et al., 2005; Santos-Rosa et al., 2002), while in vertebrates dimethylated H3K4 correlates with trimethylated H3K4 in highly active genes (Bernstein et al., 2005; Schneider et al., 2004). Genome-wide analysis of intraerythrocytic *P. falciparum* stages revealed that H3K4me3 was predominant at the intergenic regions, increasing in trophozoite and schizont stage parasites, in which transcription peaks (Bártfai et al., 2010).

In *P. falciparum*, the H3K4 mark colocalizes almost perfectly with the histone variant H2A.Z and histone H3K9ac (Bártfai et al., 2010). Interestingly, the histone variant H2A.Z is absent from subtelomeric and chromosome internal heterochromatic islands, in which *var* genes reside, and is complemented by H2A occupancy (Bártfai et al., 2010). Importantly in this context, transcriptional activation of a *var* gene requires a histone variant exchange at its promoter, during which H2A is replaced by H2A.Z (Petter et al., 2011). With the initiation of the S phase-dependent silencing of *var* genes, H2A.Z is lost from the promoter (Petter et al., 2011) possibly through deposition of newly synthesized canonical histones (Groth et al., 2007). While histones can be already largely acetylated prior to nucleosome assembly (Corpet and Almouzni, 2009), they generally lack methylation marks (Loyola et al., 2006). In our study, we observed that H3K4me3 levels, besides H3K4me2 and H3K9ac levels, are similarly high on an active compared to a "poised" *var* promoter, which is marked for reactivation in the next generation. This is consistent with the hypothesis that PfSET10 is the HKMT responsible for H3K4 methylation of the newly assembled nucleosome at the *var* promoter following replication, thereby maintaining a poised *var* promoter state. The recruitment of PfSET10 to its target site may be determined through DNA-specific binding factors, components of the transcription machinery or RNA (Ruthenburg et al., 2007), and with its PHD finger binding the unmethylated form of lysine 4 of a freshly deposited histone H3.

Previous studies have demonstrated that proteins specific for *var* gene regulation can be either amenable or refractory to genetic deletion (Duraisingh et al., 2005; Flueck et al., 2009; Tonkin et al., 2009). PfSET10 appears to be essential for parasite survival, since we were unable to obtain parasites in which PfSET10 has been disrupted. PfSET10 marks a transcription site and appears responsible for H3K4 methylation. Although it is not known at this stage how many genes utilize this site for transcription, PfSET10 removal would likely cause parasite lethality if expression of essential proteins is affected.

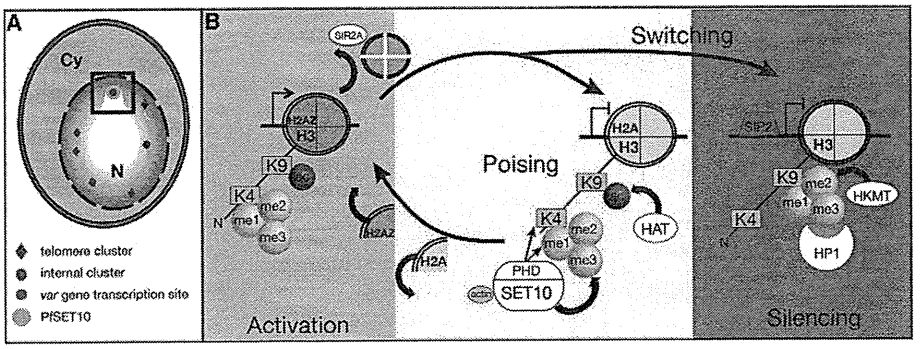

Figure 6. A Proposed Model for the Role of PfSET10 in Regulation of the Active *var* Gene in the Expression Site at the Nuclear Periphery

(A) PfSET10 localizes to the subnuclear region into which *var* genes are translocated for expression. Cy, cytoplasm in light brown; N, nucleus; the white area represents the euchromatic central part and subnuclear *var* gene expression site, while the gray area represents the heterochromatic nuclear periphery. A black square highlights the subnuclear expression site in which PfSET10 resides.

(B) Schematic presentation of histone H3 epigenetic modifications involved in *var* gene regulation and the proposed role of PfSET10. *Var* gene transcription associates with an open chromatin structure characterized by H3K4 trimethylation, H3K9 acetylation, and histone variant H2AZ. S phase dependent silencing of *var* genes is consistent with loss of histone variant H2AZ from the active *var* promoter. After replication, canonical histones such as histone H2A and H3 are incorporated to the *var* promoter providing a window of opportunity for switching and silencing. For poising, PfSET10 binds to non-or monomethylated H3K4, where it most likely sets the di- and trimethyl mark. This epigenetic profile is maintained during division and likely enables activation in daughter cells. Histone H2.AZ is deposited at the *var* promoter during ring stage. *Var* gene silencing involves movement of the *var* gene locus out of the expression site, deacetylation likely mediated by SIR2 homologs and H3K9 trimethylation by a yet unknown HKMT. PfSIP2 and PfHP1 are required for formation of stable heterochromatin. The color code used represents *green* for activation, *yellow* for poising and *red* for silencing.

Alternatively, absence of PfSET10 may lead to alterations in local chromatin structure, which in turn might affect chromosome organization and function. Already, the tagging of GFP to the endogenous *pfset10* locus led to changes in chromatin structure at the active and poised *var* gene locus and to altered levels of H3K4 methylation. Since the localization of the PfSET10-GFP is comparable to that of the HA-tagged protein, this increased H3K4 methylation could be the result of increased activity of the tagged PfSET10 and might account for the altered *var* gene transcription pattern. Alternatively, the GFP-tag of PfSET10 could interfere with the binding of a yet unknown transcriptional repressor, leading to a higher level of *var* transcription and consequently higher level of H3K4 methylation.

Modifications of core histones are involved in chromatin remodeling and gene regulation. Methylation of histones is thought to be important for heritable transmission of epigenetic information (memory) through cell division (Muramoto et al., 2010). PfSET10 is a *P. falciparum* histone 3 lysine 4 methyltransferase that defines the transcriptional zone into which a *var* gene is translocated for activation (Figure 6). The "active" *var* gene is activated in early ring stages and the resulting transcript translated into PfEMP1, followed by translocation to the infected erythrocyte membrane surface. This *var* gene is maintained in a poised state during cell division, ready for activation in the daughter cells of the next *P. falciparum* cycle. PfSET10 is likely required for the maintenance of the transcriptionally permissive chromatin environment of the active *var* promoter through division, by methylating the freshly incorporated histone H3, and involved in memory for the heritable transmission of epigenetic information during cell division. Our study has identified PfSET10 as a component of the *var* gene expression site and identifies it as an important regulator of virulence and phenotypic variation in *P. falciparum*, an important infectious agent of humans.

EXPERIMENTAL PROCEDURES

See a detailed version in Supplemental Information.

Parasite Culture and Transfection

PCR amplification was performed on *P. falciparum* strain 3D7 genomic DNA to obtain *Pfset10* 3′, which was cloned into a hemagglutinin (HA) vector, containing the human dihydrofolate reductase (*hdhfr*) gene (Crabb and Cowman, 1996; Fidock and Wellems, 1997), or into the GFP-FKBP-fusion or HA-FKBP-fusion vector, respectively, for conditional knockout construct generation (Armstrong and Goldberg, 2007; Fidock and Wellems, 1997). For gene deletion, PCR amplification was performed to obtain *Pfset10* 5′ and *Pfset10* 3′ fragments, which were cloned to the pCC4 vector (Maier et al., 2008). Primers are listed in Table S1.

P. falciparum 3D7 parasites were cultured and transfected as described (Crabb and Cowman, 1996; Armstrong and Goldberg, 2007). Integration of the 3′ gene replacement constructs was by homologous recombination (Figures S1 and S5). 3D7SET10-HA and 3D7 samples were analyzed by western blot, and PFSET10-HA was detected with anti-HA antibody.

Recombinant Protein Expression

The PfSET10 fragment containing SET and PHD finger domains was codon-optimized for wheat and synthesized (Epoch Biolabs, Inc.) and expressed in a wheat germ cell-free expression system (Cell-Free Sciences) (Tsuboi et al., 2010). The in vitro histone peptide-binding assay was performed with a Biotinylated Protein-Protein Pull-Down Kit (Pierce).

Far Western

P. falciparum histones were run on a 4%–12% Bis-Tris gel, and the membrane was incubated with 2 μg/ml of recombinant protein and anti-His and secondary antibody, then detected using Amersham ECL Western Blotting Detection Reagent (GE Healthcare).

HMKT Assay

To purify HA-tagged, full-length PfSET10 protein from 3D7SET10-HA and 3D7 parasites, 2×10^9 late-stage parasites were harvested, and cell extracts were prepared. HA-tagged PfSET10 was purified by anti-HA beads (Sigma). The in vitro histone methyltransferase assay was performed as described (Fingerman et al., 2008).

Nuclear Fractionation

Nuclear and cytoplasmic protein fractions from 3D7SET10-HA parasites were obtained as described (Voss et al., 2002), analyzed by western blot, and *Pf*SET10-HA was detected with anti-HA antibody.

Fluorescence Microscopy, Combined IFA/FISH and Transmission Electron Microscopy

Methanol-fixed cells were analyzed using mouse anti-HA 3F10 (Roche), anti-H3K4m1 (Abcam, ab8895), anti-H3K4m2 (Abcam, ab7766), anti-H3K4m3 (upstate, 05-745), anti-H3K9ac (upstate, 06-942), anti-H3K9m3 (Abcam, ab8898), anti-histone H2A (abcam, ab18255), anti-PfH2.AZ (Petter et al., 2011), anti-PfHP1 (Petter et al., 2011), anti-PfActin-1 (Riglar et al., 2011), and Alexa Fluor 488 conjugated anti-mouse IgG (Molecular Probes). IFA/FISH was carried out as described (Flueck et al., 2009). Statistical analysis was performed using a two-sided, two-sample Kolmogorov-Smirnov test. Immunoelectron microscopy was performed on 3D7SET10-HA schizonts, which were fixed (4% formaldehyde, 0.1% glutaraldehyde), dehydrated, and embedded in LR Gold resin (Electron Microscopy Sciences, Fort Washington, PA).

Chromatin Immunoprecipitation (ChIP) and Transcriptional Profiling

ChIP analysis was performed as described (Flueck et al., 2009). Primers are listed in Table S1. RNA was harvested by cell lysis in TRIzol (Invitrogen), purified as described (Kyes et al., 2000), and cDNA was generated using Superscript III Reverse Transcriptase (Invitrogen). Quantitative RT-PCR was performed as described (Duffy et al., 2009; Petter et al., 2011). Primers are listed in Table S1.

Protein Pull-Down

HA-tagged, full-length *Pf*SET10 protein and interacting proteins from 3D7/*Pf*SET10HA and control line 3D7 were purified using anti-HA beads (Sigma). Proteins were separated on a SDS-PAGE and stained in colloidal Coomassie. Protein bands were excised and submitted for LC-MS/MS analysis. After separation of the pull-down fraction in SDS-PAGE, membranes were probed with either anti-HA 3F10 (Roche) or anti-PfActin-1 (Riglar et al., 2011).

CSA Binding Assay

Enrichment of parasites expressing *var2csa* PfEMP1 or PFL0020w PfEMP1 through subsequent CSA- or ICAM-binding assays was performed as described (Duraisingh et al., 2005).

SUPPLEMENTAL INFORMATION

Supplemental Information includes six figures, two tables, Supplemental Experimental Procedures, and Supplemental References and can be found online with this article at doi:10.1016/j.chom.2011.11.011.

ACKNOWLEDGMENTS

We thank Stefan Glaser (WEHI, Melbourne) for helpful discussions and the Red Cross Blood Service (Australia) for blood. This work was supported by the National Health and Medical Research Council of Australia (NHMRC). A.F.C. is an Australia Fellow of the NHMRC. This work was made possible through Victorian State Government Operational Infrastructure Support and Australian Government NHMRC IRIISS. J.C.V. was supported by a HFSP long-term fellowship. Work in the Stunnenberg laboratory was supported by EVIMalaR.

Received: May 10, 2011
Revised: October 27, 2011
Accepted: November 30, 2011
Published: January 18, 2012

REFERENCES

Armstrong, C.M., and Goldberg, D.E. (2007). An FKBP destabilization domain modulates protein levels in *Plasmodium falciparum*. Nat. Methods *4*, 1007–1009.

Barnwell, J.W. (1989). Cytoadherence and sequestration in falciparum malaria. Exp. Parasitol. *69*, 407–412.

Bártfai, R., Hoeijmakers, W.A., Salcedo-Amaya, A.M., Smits, A.H., Janssen-Megens, E., Kaan, A., Treeck, M., Gilberger, T.W., Françoijs, K.J., and Stunnenberg, H.G. (2010). H2A.Z demarcates intergenic regions of the *plasmodium falciparum* epigenome that are dynamically marked by H3K9ac and H3K4me3. PLoS Pathog. *6*, e1001223.

Baruch, D.I., Pasloske, B.L., Singh, H.B., Bi, X., Ma, X.C., Feldman, M., Taraschi, T.F., and Howard, R.J. (1995). Cloning the *P. falciparum* gene encoding PfEMP1, a malarial variant antigen and adherence receptor on the surface of parasitized human erythrocytes. Cell *82*, 77–87.

Berendt, A.R., Simmons, D.L., Tansey, J., Newbold, C.I., and Marsh, K. (1989). Intercellular adhesion molecule-1 is an endothelial cell adhesion receptor for Plasmodium falciparum. Nature *341*, 57–59.

Bernstein, B.E., Humphrey, E.L., Erlich, R.L., Schneider, R., Bouman, P., Liu, J.S., Kouzarides, T., and Schreiber, S.L. (2002). Methylation of histone H3 Lys 4 in coding regions of active genes. Proc. Natl. Acad. Sci. USA *99*, 8695–8700.

Bernstein, B.E., Kamal, M., Lindblad-Toh, K., Bekiranov, S., Bailey, D.K., Huebert, D.J., McMahon, S., Karlsson, E.K., Kulbokas, E.J., 3rd, Gingeras, T.R., et al. (2005). Genomic maps and comparative analysis of histone modifications in human and mouse. Cell *120*, 169–181.

Briggs, S.D., Bryk, M., Strahl, B.D., Cheung, W.L., Davie, J.K., Dent, S.Y., Winston, F., and Allis, C.D. (2001). Histone H3 lysine 4 methylation is mediated by Set1 and required for cell growth and rDNA silencing in *Saccharomyces cerevisiae*. Genes Dev. *15*, 3286–3295.

Brown, K.E., Guest, S.S., Smale, S.T., Hahm, K., Merkenschlager, M., and Fisher, A.G. (1997). Association of transcriptionally silent genes with Ikaros complexes at centromeric heterochromatin. Cell *91*, 845–854.

Brown, K.E., Baxter, J., Graf, D., Merkenschlager, M., and Fisher, A.G. (1999). Dynamic repositioning of genes in the nucleus of lymphocytes preparing for cell division. Mol. Cell *3*, 207–217.

Bull, P.C., Lowe, B.S., Kortok, M., Molyneux, C.S., Newbold, C.I., and Marsh, K. (1998). Parasite antigens on the infected red cell surface are targets for naturally acquired immunity to malaria. Nat. Med. *4*, 358–360.

Chuang, C.H., Carpenter, A.E., Fuchsova, B., Johnson, T., de Lanerolle, P., and Belmont, A.S. (2006). Long-range directional movement of an interphase chromosome site. Curr. Biol. *16*, 825–831.

Cooke, B.M., and Coppel, R.L. (1995). Cytoadhesion and falciparum malaria: going with the flow. Parasitol. Today (Regul. Ed.) *11*, 282–287.

Corpet, A., and Almouzni, G. (2009). Making copies of chromatin: the challenge of nucleosomal organization and epigenetic information. Trends Cell Biol. *19*, 29–41.

Crabb, B.S., and Cowman, A.F. (1996). Characterization of promoters and stable transfection by homologous and nonhomologous recombination in *Plasmodium falciparum*. Proc. Natl. Acad. Sci. USA *93*, 7289–7294.

Cui, L., and Miao, J. (2010). Chromatin-mediated epigenetic regulation in the malaria parasite *Plasmodium falciparum*. Eukaryot. Cell *9*, 1138–1149.

Cui, L., Fan, Q., Cui, L., and Miao, J. (2008). Histone lysine methyltransferases and demethylases in *Plasmodium falciparum*. Int. J. Parasitol. *38*, 1083–1097.

Dillon, S.C., Zhang, X., Trievel, R.C., and Cheng, X. (2005). The SET-domain protein superfamily: protein lysine methyltransferases. Genome Biol. *6*, 227.

Duffy, M.F., Byrne, T.J., Carret, C., Ivens, A., and Brown, G.V. (2009). Ectopic recombination of a malaria *var* gene during mitosis associated with an altered var switch rate. J. Mol. Biol. *389*, 453–469.

Dundr, M., Ospina, J.K., Sung, M.H., John, S., Upender, M., Ried, T., Hager, G.L., and Matera, A.G. (2007). Actin-dependent intranuclear repositioning of an active gene locus *in vivo*. J. Cell Biol. *179*, 1095–1103.

Duraisingh, M.T., Voss, T.S., Marty, A.J., Duffy, M.F., Good, R.T., Thompson, J.K., Freitas-Junior, L.H., Scherf, A., Crabb, B.S., and Cowman, A.F. (2005). Heterochromatin silencing and locus repositioning linked to regulation of virulence genes in *Plasmodium falciparum*. Cell *121*, 13–24.

Dzikowski, R., Frank, M., and Deitsch, K. (2006). Mutually exclusive expression of virulence genes by malaria parasites is regulated independently of antigen production. PLoS Pathog. *2*, e22.

Dzikowski, R., Li, F., Amulic, B., Eisberg, A., Frank, M., Patel, S., Wellems, T.E., and Deitsch, K.W. (2007). Mechanisms underlying mutually exclusive expression of virulence genes by malaria parasites. EMBO Rep. *8*, 959–965.

Fidock, D.A., and Wellems, T.E. (1997). Transformation with human dihydrofolate reductase renders malaria parasites insensitive to WR99210 but does not affect the intrinsic activity of proguanil. Proc. Natl. Acad. Sci. USA *94*, 10931–10936.

Fingerman, I.M., Du, H.N., and Briggs, S.D. (2008). In vitro histone methyltransferase assay. CSH Protoc *2008*, pdb.prot4939.

Flueck, C., Bartfai, R., Volz, J., Niederwieser, I., Salcedo-Amaya, A.M., Alako, B.T., Ehlgen, F., Ralph, S.A., Cowman, A.F., Bozdech, Z., et al. (2009). *Plasmodium falciparum* heterochromatin protein 1 marks genomic loci linked to phenotypic variation of exported virulence factors. PLoS Pathog. *5*, e1000569.

Freitas-Junior, L.H., Bottius, E., Pirrit, L.A., Deitsch, K.W., Scheidig, C., Guinet, F., Nehrbass, U., Wellems, T.E., and Scherf, A. (2000). Frequent ectopic recombination of virulence factor genes in telomeric chromosome clusters of *P. falciparum*. Nature *407*, 1018–1022.

Freitas-Junior, L.H., Hernandez-Rivas, R., Ralph, S.A., Montiel-Condado, D., Ruvalcaba-Salazar, O.K., Rojas-Meza, A.P., Mâncio-Silva, L., Leal-Silvestre, R.J., Gontijo, A.M., Shorte, S., and Scherf, A. (2005). Telomeric heterochromatin propagation and histone acetylation control mutually exclusive expression of antigenic variation genes in malaria parasites. Cell *121*, 25–36.

Gardner, M.J., Hall, N., Fung, E., White, O., Berriman, M., Hyman, R.W., Carlton, J.M., Pain, A., Nelson, K.E., Bowman, S., et al. (2002). Genome sequence of the human malaria parasite *Plasmodium falciparum*. Nature *419*, 498–511.

Glaser, S., Schaft, J., Lubitz, S., Vintersten, K., van der Hoeven, F., Tufteland, K.R., Aasland, R., Anastassiadis, K., Ang, S.L., and Stewart, A.F. (2006). Multiple epigenetic maintenance factors implicated by the loss of Mll2 in mouse development. Development *133*, 1423–1432.

Groth, A., Rocha, W., Verreault, A., and Almouzni, G. (2007). Chromatin challenges during DNA replication and repair. Cell *128*, 721–733.

Howitt, C.A., Wilinski, D., Llinás, M., Templeton, T.J., Dzikowski, R., and Deitsch, K.W. (2009). Clonally variant gene families in *Plasmodium falciparum* share a common activation factor. Mol. Microbiol. *73*, 1171–1185.

Jackson, D.A., Hassan, A.B., Errington, R.J., and Cook, P.R. (1993). Visualization of focal sites of transcription within human nuclei. EMBO J. *12*, 1059–1065.

Krogan, N.J., Dover, J., Khorrami, S., Greenblatt, J.F., Schneider, J., Johnston, M., and Shilatifard, A. (2002). COMPASS, a histone H3 (Lysine 4) methyltransferase required for telomeric silencing of gene expression. J. Biol. Chem. *277*, 10753–10755.

Kyes, S.A., Rowe, J.A., Kriek, N., and Newbold, C.I. (1999). Rifins: a second family of clonally variant proteins expressed on the surface of red cells infected with *Plasmodium falciparum*. Proc. Natl. Acad. Sci. USA *96*, 9333–9338.

Kyes, S., Pinches, R., and Newbold, C. (2000). A simple RNA analysis method shows var and rif multigene family expression patterns in *Plasmodium falciparum*. Mol. Biochem. Parasitol. *105*, 311–315.

Lan, F., Bayliss, P.E., Rinn, J.L., Whetstine, J.R., Wang, J.K., Chen, S., Iwase, S., Alpatov, R., Issaeva, I., Canaani, E., et al. (2007). A histone H3 lysine 27 demethylase regulates animal posterior development. Nature *449*, 689–694.

Lavazec, C., Sanyal, S., and Templeton, T.J. (2007). Expression switching in the stevor and Pfmc-2TM superfamilies in *Plasmodium falciparum*. Mol. Microbiol. *64*, 1621–1634.

Lee, S., Lee, D.K., Dou, Y., Lee, J., Lee, B., Kwak, E., Kong, Y.Y., Lee, S.K., Roeder, R.G., and Lee, J.W. (2006). Coactivator as a target gene specificity determinant for histone H3 lysine 4 methyltransferases. Proc. Natl. Acad. Sci. USA *103*, 15392–15397.

Leech, J.H., Barnwell, J.W., Miller, L.H., and Howard, R.J. (1984). Identification of a strain-specific malarial antigen exposed on the surface of *Plasmodium falciparum*-infected erythrocytes. J. Exp. Med. *159*, 1567–1575.

Lopez-Rubio, J.J., Gontijo, A.M., Nunes, M.C., Issar, N., Hernandez Rivas, R., and Scherf, A. (2007). 5′ flanking region of *var* genes nucleate histone modification patterns linked to phenotypic inheritance of virulence traits in malaria parasites. Mol. Microbiol. *66*, 1296–1305.

Loyola, A., Bonaldi, T., Roche, D., Imhof, A., and Almouzni, G. (2006). PTMs on H3 variants before chromatin assembly potentiate their final epigenetic state. Mol. Cell *24*, 309–316.

MacPherson, G.G., Warrell, M.J., White, N.J., Looareesuwan, S., and Warrell, D.A. (1985). Human cerebral malaria. A quantitative ultrastructural analysis of parasitized erythrocyte sequestration. Am. J. Pathol. *119*, 385–401.

Maier, A.G., Rug, M., O'Neill, M.T., Brown, M., Chakravorty, S., Szestak, T., Chesson, J., Wu, Y., Hughes, K., Coppel, R.L., et al. (2008). Exported proteins required for virulence and rigidity of *Plasmodium falciparum*-infected human erythrocytes. Cell *134*, 48–61.

Mellor, J. (2006). It takes a PHD to read the histone code. Cell *126*, 22–24.

Muramoto, T., Müller, I., Thomas, G., Melvin, A., and Chubb, J.R. (2010). Methylation of H3K4 Is required for inheritance of active transcriptional states. Curr. Biol. *20*, 397–406.

Nagy, P.L., Griesenbeck, J., Kornberg, R.D., and Cleary, M.L. (2002). A trithorax-group complex purified from *Saccharomyces cerevisiae* is required for methylation of histone H3. Proc. Natl. Acad. Sci. USA *99*, 90–94.

Newbold, C.I., Craig, A.G., Kyes, S., Berendt, A.R., Snow, R.W., Peshu, N., and Marsh, K. (1997). PfEMP1, polymorphism and pathogenesis. Ann. Trop. Med. Parasitol. *91*, 551–557.

Ng, H.H., Robert, F., Young, R.A., and Struhl, K. (2003). Targeted recruitment of Set1 histone methylase by elongating Pol II provides a localized mark and memory of recent transcriptional activity. Mol. Cell *11*, 709–719.

Niang, M., Yan Yam, X., and Preiser, P.R. (2009). The *Plasmodium falciparum* STEVOR multigene family mediates antigenic variation of the infected erythrocyte. PLoS Pathog. *5*, e1000307.

Ockenhouse, C.F., Tegoshi, T., Maeno, Y., Benjamin, C., Ho, M., Kan, K.E., Thway, Y., Win, K., Aikawa, M., and Lobb, R.R. (1992). Human vascular endothelial cell adhesion receptors for *Plasmodium falciparum*-infected erythrocytes: roles for endothelial leukocyte adhesion molecule 1 and vascular cell adhesion molecule 1. J. Exp. Med. *176*, 1183–1189.

Org, T., Chignola, F., Hetényi, C., Gaetani, M., Rebane, A., Liiv, I., Maran, U., Mollica, L., Bottomley, M.J., Musco, G., and Peterson, P. (2008). The autoimmune regulator PHD finger binds to non-methylated histone H3K4 to activate gene expression. EMBO Rep. *9*, 370–376.

Osborne, C.S., Chakalova, L., Brown, K.E., Carter, D., Horton, A., Debrand, E., Goyenechea, B., Mitchell, J.A., Lopes, S., Reik, W., and Fraser, P. (2004). Active genes dynamically colocalize to shared sites of ongoing transcription. Nat. Genet. *36*, 1065–1071.

Petter, M., Lee, C.C., Byrne, T.J., Boysen, K.E., Volz, J., Ralph, S.A., Cowman, A.F., Brown, G.V., and Duffy, M.F. (2011). Expression of *P. falciparum var* genes involves exchange of the histone variant H2A.Z at the promoter. PLoS Pathog. *7*, e1001292.

Pokholok, D.K., Harbison, C.T., Levine, S., Cole, M., Hannett, N.M., Lee, T.I., Bell, G.W., Walker, K., Rolfe, P.A., Herbolsheimer, E., et al. (2005). Genome-wide map of nucleosome acetylation and methylation in yeast. Cell *122*, 517–527.

Ralph, S.A., Scheidig-Benatar, C., and Scherf, A. (2005). Antigenic variation in *Plasmodium falciparum* is associated with movement of *var* loci between subnuclear locations. Proc. Natl. Acad. Sci. USA *102*, 5414–5419.

Raventos-Suarez, C., Kaul, D.K., Macaluso, F., and Nagel, R.L. (1985). Membrane knobs are required for the microcirculatory obstruction induced by *Plasmodium falciparum*-infected erythrocytes. Proc. Natl. Acad. Sci. USA *82*, 3829–3833.

Riglar, D.T., Richard, D., Wilson, D.W., Boyle, M.J., Dekiwadia, C., Turnbull, L., Angrisano, F., Marapana, D.S., Rogers, K.L., Whitchurch, C.B., et al. (2011). Super-resolution dissection of coordinated events during malaria parasite invasion of the human erythrocyte. Cell Host Microbe *9*, 9–20.

Rogerson, S.J., Chaiyaroj, S.C., Ng, K., Reeder, J.C., and Brown, G.V. (1995). Chondroitin sulfate A is a cell surface receptor for *Plasmodium falciparum*-infected erythrocytes. J. Exp. Med. *182*, 15–20.

Roguev, A., Schaft, D., Shevchenko, A., Pijnappel, W.W., Wilm, M., Aasland, R., and Stewart, A.F. (2001). The *Saccharomyces cerevisiae* Set1 complex includes an *Ash2* homologue and methylates histone 3 lysine 4. EMBO J. *20*, 7137–7148.

Ruthenburg, A.J., Allis, C.D., and Wysocka, J. (2007). Methylation of lysine 4 on histone H3: intricacy of writing and reading a single epigenetic mark. Mol. Cell *25*, 15–30.

Salanti, A., Staalsoe, T., Lavstsen, T., Jensen, A.T., Sowa, M.P., Arnot, D.E., Hviid, L., and Theander, T.G. (2003). Selective upregulation of a single distinctly structured *var* gene in chondroitin sulphate A-adhering *Plasmodium falciparum* involved in pregnancy-associated malaria. Mol. Microbiol. *49*, 179–191.

Santos-Rosa, H., Schneider, R., Bannister, A.J., Sherriff, J., Bernstein, B.E., Emre, N.C., Schreiber, S.L., Mellor, J., and Kouzarides, T. (2002). Active genes are tri-methylated at K4 of histone H3. Nature *419*, 407–411.

Schneider, R., Bannister, A.J., Myers, F.A., Thorne, A.W., Crane-Robinson, C., and Kouzarides, T. (2004). Histone H3 lysine 4 methylation patterns in higher eukaryotic genes. Nat. Cell Biol. *6*, 73–77.

Schübeler, D., Francastel, C., Cimbora, D.M., Reik, A., Martin, D.I., and Groudine, M. (2000). Nuclear localization and histone acetylation: a pathway for chromatin opening and transcriptional activation of the human beta-globin locus. Genes Dev. *14*, 940–950.

Smith, J.D., Chitnis, C.E., Craig, A.G., Roberts, D.J., Hudson-Taylor, D.E., Peterson, D.S., Pinches, R., Newbold, C.I., and Miller, L.H. (1995). Switches in expression of *Plasmodium falciparum* var genes correlate with changes in antigenic and cytoadherent phenotypes of infected erythrocytes. Cell *82*, 101–110.

Su, X.Z., Heatwole, V.M., Wertheimer, S.P., Guinet, F., Herrfeldt, J.A., Peterson, D.S., Ravetch, J.A., and Wellems, T.E. (1995). The large diverse gene family *var* encodes proteins involved in cytoadherence and antigenic variation of *Plasmodium falciparum*-infected erythrocytes. Cell *82*, 89–100.

Tonkin, C.J., Carret, C.K., Duraisingh, M.T., Voss, T.S., Ralph, S.A., Hommel, M., Duffy, M.F., Silva, L.M., Scherf, A., Ivens, A., et al. (2009). Sir2 paralogues cooperate to regulate virulence genes and antigenic variation in *Plasmodium falciparum*. PLoS Biol. *7*, e84.

Trievel, R.C., Beach, B.M., Dirk, L.M., Houtz, R.L., and Hurley, J.H. (2002). Structure and catalytic mechanism of a SET domain protein methyltransferase. Cell *111*, 91–103.

Tsuboi, T., Takeo, S., Sawasaki, T., Torii, M., and Endo, Y. (2010). An efficient approach to the production of vaccines against the malaria parasite. Methods Mol. Biol. *607*, 73–83.

Visa, N., and Percipalle, P. (2010). Nuclear functions of actin. Cold Spring Harb Perspect Biol *2*, a000620.

Volz, J., Carvalho, T.G., Ralph, S.A., Gilson, P., Thompson, J., Tonkin, C.J., Langer, C., Crabb, B.S., and Cowman, A.F. (2010). Potential epigenetic regulatory proteins localise to distinct nuclear sub-compartments in *Plasmodium falciparum*. Int. J. Parasitol. *40*, 109–121.

Voss, T.S., Mini, T., Jenoe, P., and Beck, H.P. (2002). *Plasmodium falciparum* possesses a cell cycle-regulated short type replication protein A large subunit encoded by an unusual transcript. J. Biol. Chem. *277*, 17493–17501.

Voss, T.S., Healer, J., Marty, A.J., Duffy, M.F., Thompson, J.K., Beeson, J.G., Reeder, J.C., Crabb, B.S., and Cowman, A.F. (2006). A *var* gene promoter controls allelic exclusion of virulence genes in *Plasmodium falciparum* malaria. Nature *439*, 1004–1008.

Wahlgren, M., Fernandez, V., Scholander, C., and Carlson, J. (1994). Rosetting. Parasitol. Today (Regul. Ed.) *10*, 73–79.

Wang, J., Shiels, C., Sasieni, P., Wu, P.J., Islam, S.A., Freemont, P.S., and Sheer, D. (2004). Promyelocytic leukemia nuclear bodies associate with transcriptionally active genomic regions. J. Cell Biol. *164*, 515–526.

Weiner, A., Dahan-Pasternak, N., Shimoni, E., Shinder, V., von Huth, P., Elbaum, M., and Dzikowski, R. (2011). 3D nuclear architecture reveals coupled cell cycle dynamics of chromatin and nuclear pores in the malaria parasite *Plasmodium falciparum*. Cell. Microbiol. *13*, 967–977.

Yu, B.D., Hess, J.L., Horning, S.E., Brown, G.A., and Korsmeyer, S.J. (1995). Altered Hox expression and segmental identity in Mll-mutant mice. Nature *378*, 505–508.

Vaccine 30 (2012) 1807–1812

Contents lists available at SciVerse ScienceDirect

Vaccine

journal homepage: www.elsevier.com/locate/vaccine

Plasmodium vivax gametocyte protein Pvs230 is a transmission-blocking vaccine candidate

Mayumi Tachibana[a], Chiho Sato[a], Hitoshi Otsuki[b], Jetsumon Sattabongkot[c,1], Osamu Kaneko[d], Motomi Torii[a,e,**], Takafumi Tsuboi[e,f,g,*]

[a] Department of Molecular Parasitology, Ehime University Graduate School of Medicine, Shitsukawa, Toon, Ehime 791-0295, Japan
[b] Division of Medical Zoology, Faculty of Medicine, Tottori University, Yonago, Tottori 683-8503, Japan
[c] Department of Entomology, Armed Forces Research Institute of Medical Sciences, Bangkok 10400, Thailand
[d] Department of Protozoology, Institute of Tropical Medicine (NEKKEN) and the Global Center of Excellence Program, Nagasaki University, Sakamoto, Nagasaki 852-8523, Japan
[e] Ehime Proteo-Medicine Research Center, Ehime University, Toon, Ehime 791-0295, Japan
[f] Cell-Free Science and Technology Research Center, Ehime University, Matsuyama, Ehime 790-8577, Japan
[g] Venture Business Laboratory, Ehime University, Matsuyama, Ehime 790-8577, Japan

ARTICLE INFO

Article history:
Received 29 July 2011
Received in revised form
24 December 2011
Accepted 2 January 2012
Available online 11 January 2012

Keywords:
DNA vaccine
Gametocyte
Malaria
Plasmodium vivax
Pvs230
Transmission-blocking vaccine

ABSTRACT

The malaria transmission-blocking vaccine (TBV) aims to interfere the development of malaria parasite in the mosquito and prevent further transmission in the community. So far only two TBV candidates have been identified in *Plasmodium vivax*; ookinete surface proteins Pvs25 and Pvs28. The *pvs230* (PVX_003905) is reported as an ortholog of Pfs230, a gametocyte/gamete stage TBV candidate in *Plasmodium falciparum*, however its candidacy for TBV has never been tested. Therefore here, we have investigated whether Pvs230 can be a TBV candidate using *P. vivax* samples obtained from Thailand. The mouse antiserum raised against the plasmid expressing CRDs I–IV of Pvs230 detected Pvs230 protein in the lysate of *P. vivax* gametocyte in western blot analysis under non-reducing condition. From the localization of Pvs230 on the outer most regions of gametocyte in the immunofluorescence assay, it appears that Pvs230 is localized on the surface of gametes. Importantly, the anti-Pvs230 mouse serum significantly reduced the number of *P. vivax* oocysts developed in the mosquito midgut. Moreover, the polymorphism in Pvs230 CRDs I–IV is limited suggesting that it may not be an impediment for the utilization of Pvs230 as an effective TBV candidate. In conclusion, our results show that Pvs230 is a transmission-blocking vaccine candidate of *P. vivax*.

1. Introduction

Malaria is one of the major global public health problems which inhibit social and economic development of vast areas of the tropical regions of the world [1]. While malaria mortality is mainly due to the infection of *Plasmodium falciparum*, *Plasmodium vivax* remains to be a huge burden to the communities in Asia, Pacific, and Central and South America. The emergence of mosquito strains resistant to insecticides and parasites resistant to anti-malarial drugs is a major limiting factor making malaria eradication difficult [2,3]. Moreover, a recent study showed that though the incidence of *P. falciparum* could be eliminated by the malaria mass drug treatment in an island in Vanuatu, still the *P. vivax* cases remained [4]. Therefore, the development of vaccines against *P. vivax* is also an essential component towards malaria elimination [5].

At present there are only two leading vivax vaccine candidates in Phase I of the vaccine development pipeline [5]; circumsporozoite protein (CSP) (a pre-erythrocytic vaccine candidate which acts against sporozoites and liver-stage parasites and prevent infection) [6] and Pvs25 (a transmission-blocking vaccine (TBV) candidate which blocks malaria transmission by interrupting the parasite life cycle in the mosquito midgut) [7,8].

TBV targets the molecules of the sexual stage parasites in mosquito (i.e., gametocyte, gamete, zygote, and ookinete) and in human (gametocyte). The leading targets for TBV are ookinete surface proteins; Pfs25 in *P. falciparum* [9] and Pvs25 and Pvs28 in *P. vivax* [10]. Both Pfs25 and Pvs25 are expressed only on the surface

* Corresponding author at: Cell-Free Science and Technology Research Center, Ehime University, Matsuyama, Ehime 790-8577, Japan.
Tel.: +81 89 927 8277; fax: +81 89 927 9941.
** Corresponding author at: Department of Molecular Parasitology, Ehime University Graduate School of Medicine, Toon, Ehime 791-0295, Japan. Tel.: +81 89 960 5285; fax: +81 89 960 5287.
E-mail addresses: torii@m.ehime-u.ac.jp (M. Torii), tsuboi@ccr.ehime-u.ac.jp (T. Tsuboi).
[1] Present address: Mahidol Vivax Research Center, Faculty of Tropical Medicine, Mahidol University, Bangkok, Thailand.

0264-410X/$ – see front matter © 2012 Elsevier Ltd. All rights reserved.
doi:10.1016/j.vaccine.2012.01.003

of mosquito stage parasites (zygote and ookinete). On the other hand, Pfs230, a TBV candidate of *P. falciparum*, is expressed both in human (gametocytes) and mosquito stages (gametes) [11,12]. Pfs230 is a member of the 6-cys protein family [13], and it is predicted to have a complex tertiary structure due to the presence of fourteen cysteine-rich domains (CRDs) [14,15]. Polyclonal antibody against recombinant Pfs230 region C [amino acid positions (aa) 443–1132] expressed both in *Escherichia coli* [16] and in wheat germ cell-free system [12] exhibited transmission-blocking activity (i.e., reduced the infectivity of *P. falciparum* to mosquitoes). These evidences support the rationale to prioritize the N-terminal domain of Pfs230 as falciparum TBV candidate.

Since Pvs230 in *P. vivax* is an ortholog of Pfs230, we recently performed an evolutionary and population genetic analysis on Pvs230 gene (*pvs230*: PVX_003905) using *pvs230* nucleotide sequences of field isolates collected worldwide [17]. We found that the fourteen CRDs in Pvs230 are more conserved and less polymorphic among different *Plasmodium* species (i.e. *P. falciparum*, *P. knowlesi*, *P. cynomolgi*, *P. yoelii*, *P. berghei*, *P. chabaudi*, and *P. gallinaceum*). [17]. These results reinforce the rationale that CRDs of Pvs230 can be a target of vivax TBV. Here we report that anti-Pvs230 antibody raised by DNA immunization with a plasmid expressing CRDs I–IV of Pvs230 not only recognized the native Pvs230 protein on the western blot of *P. vivax* gametocyte lysates, but also exhibited a transmission-blocking activity on the field *P. vivax* isolates from Thailand.

2. Materials and methods

2.1. Parasite collection and DNA preparation

Genomic DNA (gDNA) was extracted as described previously [10] from Salvador 1 (Sal-1) of *P. vivax* maintained in the chimpanzee (a generous gift of Dr. William Collins, CDC, Atlanta, GA). gDNA from the following patient samples used for the membrane feeding assay were also extracted as previously described [17].

Peripheral blood was collected from volunteer *P. vivax* patients after the written informed consent in Mae Sod malaria clinic in Tak province, northwestern Thailand. A single infection of *P. vivax* was diagnosed by conventional microscopy and confirmed by nested PCR. For nested PCR, the species-specific nucleotide sequences of the 18S rRNA genes of *P. falciparum*, *P. vivax*, *P. malariae*, and *P. ovale* were amplified as described previously [18]. All research involving human subjects in this study was reviewed and approved by the Institutional Ethics Committee of the Thai Ministry of Public Health and the Human Subjects Research Review Board of the United States Army.

Firstly, the leukocytes were removed from *P. vivax* infected blood collected from Thai patients by passing the blood through CF-11 column. Secondly, the leukocyte-removed blood was subjected to Percoll density gradient centrifugation to obtain gametocyte-infected erythrocytes. The fraction containing the gametocyte-infected erythrocytes was used for immunofluorescence, and immunoblotting analyses.

2.2. Plasmid DNA construction, purification, and formulation with Vaxfectin®

Based on the previous findings that Pfs230C (aa 443–1132) (Fig. 1B) is a transmission blocking vaccine candidate [12,16], here we focused on characterizing the N-terminal domain of putative mature Pvs230 as a prime TBV candidate domain. DNA fragment encoding Pvs230 CRDs I–IV (aa 236–943) (Fig. 1A) was amplified from *P. vivax* Sal-1 strain gDNA with a sense primer, Pvs230-VR-F1 (5′-ggatccGTCTTCGACAAGGTGGACG-3′) and an antisense

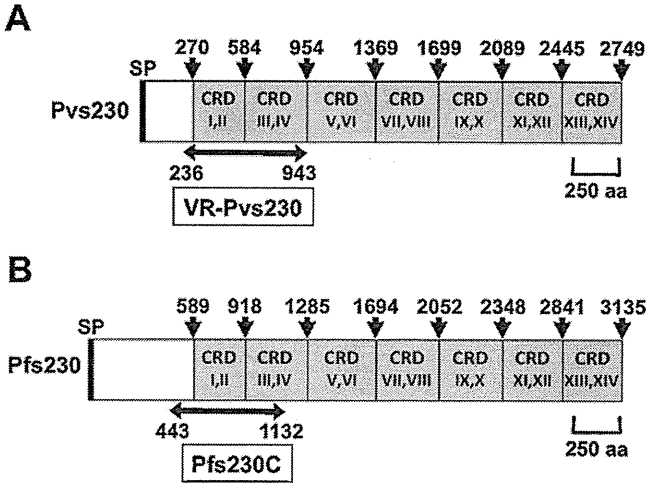

Fig. 1. Primary structure of Pvs230 and Pfs230. (A) Target regions for DNA vaccine design and RT-PCR analysis in Pvs230. SP represents signal peptide. The region comprising amino acid positions (aa) 270–2749 consists of the CRD (cysteine-rich domain) I through CRD XIV (regions shaded in gray) as described by Gerloff et al. [15]. Amino acid positions (arrows) 270, 584, 954, 1369, 1699, 2089, 2445, and 2749 indicate the starts of CRD I, III, V, VII, IX, XI, and XIII, respectively. The region that spans the domain I through domain IV (aa 236–943) was used to construct VR-Pvs230 plasmid. (B) Target region utilized for Pfs230 based TBV in the previous study [12]. SP represents a signal peptide. The region comprising amino acid positions (aa) 589–3135 consists of the CRD I through CRD XIV (regions shaded in gray) as described by Gerloff et al. [15]. Amino acid positions (arrows) 589, 918, 1285, 1694, 2052, 2348, 2841, and 3135 represent the starts of CRD I, III, V, VII, IX, XI, and XIII, respectively. Pfs230C indicates the region of Pfs230 that was tested for TBA in the previous study [12].

primer, Pvs230-VR-R1 (5′-ggatcctcaGGTTGCCTCCTGCTTCAACTC-3′) (*Bam*HI restriction site is underlined). Amplified DNA fragment was ligated into the *Bam*HI site downstream of signal sequence of tissue plasminogen activator in a eukaryotic expression vector VR1020 (Vical, Inc., San Diego, CA) to generate VR-Pvs230 plasmid expressing Pvs230 CRDs I–IV. The nucleotide sequence of the insert was confirmed using the Terminator Cycle Sequencing Kit v1.1 (Applied Biosystems, Foster City, CA) in a 310 Genetic Analyzer (Applied Biosystems). The recombinant plasmid was purified using EndoFree Plasmid Maxi Kit (Qiagen, Hilden, Germany). The plasmids were gently mixed with Vaxfectin® (Vical) in the molar ratio of 4:1 as previously described [19,20]. After 10 min incubation at room temperature, the plasmids formulated with Vaxfectin® were administered to mice within 2 h.

2.3. Production of anti-Pvs230 serum by DNA immunization

Five female DBA/2 mice in each group were immunized with 50 μg of either VR-Pvs230 (plasmid encoding aa 236–943 of Pvs230) (Fig. 1A) or VR1020 (empty plasmid vector), formulated with adjuvant Vaxfectin® by intradermal injection in the ear pinna 4 times (at 0, 3, 9, and 15 weeks) to produce anti-Pvs230 serum. Mouse antiserum was collected at 17 weeks after initial immunization. The antisera obtained from five mice in each group were pooled, heat inactivated, and stored at −80 °C until use. All animal experimental protocols were approved by the Institutional Animal Care and Use Committee of Ehime University, and the experiments were conducted according to the Ethical Guidelines for Animal Experiments of Ehime University.

2.4. Western blot analysis

The parasite proteins were extracted from gametocyte-enriched pellets of *P. vivax* Thai isolates in non-reducing SDS-PAGE loading

buffer, incubated at 95 °C for 3 min, and subjected to electrophoresis on a 7.5% polyacrylamide gel (ATTO, Tokyo, Japan). Proteins were then transferred to a 0.22-μm PVDF membrane (Bio-Rad, Hercules, CA). The membrane was blocked with Blocking One (Nacalai Tesque, Kyoto, Japan), and then incubated with mouse antiserum diluted 1:100 in phosphate buffered saline containing 0.1% Tween 20 (PBST) for 1 h. After washing the blot 3 times in PBST, the membrane was incubated for 30 min with HRP-conjugated goat anti-mouse IgG antibody (Invitrogen) diluted 1:25,000 in PBST. After washing the membrane 3 times with PBST, the proteins on the blot were visualized with Immobilon Western Chemiluminescent HRP Substrate (Millipore, Billerica, MA) on RX-U film (FujiFilm, Tokyo, Japan). The relative molecular mass of the protein was estimated with reference to Precision Plus Protein Standards (BioRad).

2.5. Indirect immunofluorescence assay (IFA)

The gametocyte-enriched fraction was spotted onto multiwell slides and acetone-fixed for immunofluorescence assay. The slides were blocked with 5% skimmed milk in PBS at 37 °C for 30 min and incubated with mouse antiserum (1:50) at 37 °C for 1 h. After washing with ice-cold PBS, the slides were incubated with Alexa Fluor® 488 goat anti-mouse IgG (H + L) antibody (1:500; Invitrogen) and nuclear stain 4′,6-Diamidino-2-phenylindole dihydrochloride (DAPI) at 37 °C for 30 min. After washing with ice-cold PBS, the slides were mounted using a ProLong antifade kit (Invitrogen) and images were obtained using fluorescent microscopy (Axiovert200, Carl Zeiss MicroImaging, Thornwood, NY) and confocal scanning laser microscopy (LSM5 Pascal, Carl Zeiss, MicroImaging).

2.6. Transmission-blocking assay

Heat-inactivated mouse antiserum was diluted with unheated (complement plus) or heat-inactivated (complement minus) AB+ human serum from malaria naïve Thai volunteers in the ratio of 1:1. These diluted serum samples were then mixed with *P. vivax*-infected erythrocytes from the patients (1:1, v/v ratio) and incubated at room temperature for 15 min. The reconstituted blood samples were introduced into membrane feeders kept at 37 °C. The starved *Anopheles dirus* mosquitoes (Bangkok colony, Armed Forces Research Institute of Medical Sciences, Thailand) were allowed to feed on the sample through the membrane feeder for 30 min. Only fully engorged mosquitoes were maintained for a week with 10% sucrose in the insectary. Twenty mosquitoes for each group were dissected and analyzed by staining with 0.5% Mercurochrome to count the number of oocysts developed within the mosquito midgut under the light microscope. Mann–Whitney *U* test was used to examine the differences in effect on the oocyst counts per mosquito by anti-VR1020 (control) and anti-VR-Pvs230 sera. Infection rate of mosquitoes was calculated as the percentage of oocyst positive mosquitoes out of the total mosquitoes dissected. The difference of the infection rate between control and Pvs230 groups was statistically analyzed by Fisher's exact test. Probability values (*P*) of less than 0.05 were considered statistically significant in both analyses.

2.7. Analysis of Polymorphism in Pvs230 CRDs I–IV

DNA fragment encoding Pvs230 CRDs I–IV (aa 236–943) (Fig. 1A) was amplified by PCR from gDNA isolated from *P. vivax* used for the membrane feeding assay with primers designed based on Sal-1 Pvs230 sequence. Primers used are sense Pvs230-30-F (5′-CAGCGATATGGTGATCACC-3′; anneals to nucleotide positions 486–504) and antisense Pvs230-31-R (5′-GCAGGTGTTCTTCACATAGC-3′; anneals to nucleotide positions 2940–2921). For sequencing, the amplified DNA fragment was directly sequenced using the Terminator Cycle Sequencing Kit v1.1 (Applied Biosystems) in a 3100 Genetic Analyzer (Applied Biosystems) as previously described [17].

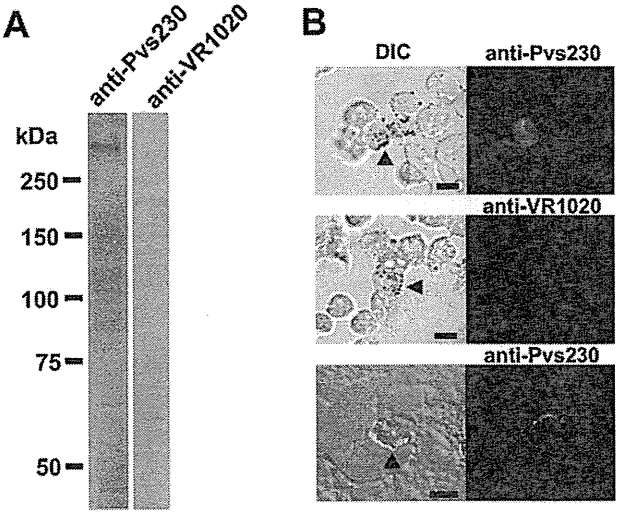

Fig. 2. Expression and localization of *pvs230* gene products. (A) Western blot analysis of Pvs230 in the extract from gametocyte-enriched *P. vivax* under non-reducing condition. Lane 1 indicates the probing with mouse anti-Pvs230 serum (anti-Pvs230). Lane 2 indicates the probing with mouse serum produced with an empty plasmid (anti-VR1020) as a negative control. (B) Reactivity of anti-Pvs230 serum by immunofluorescence microscopy. Samples enriched with gametocytes of *P. vivax* were immunostained with anti-Pvs230 serum (top and bottom panels) or antiserum against empty plasmid VR1020 (middle panels). Immunostained images (right panels) were visualized with Alexa Fluor 488-conjugated goat anti-mouse IgG (green). Nuclei were stained with DAPI (blue). The images were obtained with a conventional fluorescence microscope (top and middle panels) or with a confocal microscope (bottom panels). The left panels were the differential interference contrast images (DIC) of the samples in the respective right panels. Gametocytes were marked by arrowheads. The other cells with DAPI-positive nuclei were considered as asexual stage parasites. Scale bars, 5 μm. (For interpretation of the references to color in this figure legend, the reader is referred to the web version of the article.)

3. Results

3.1. Expression of Pvs230 in the gametocyte of P. vivax

To investigate the protein expression and the localization of Pvs230, mouse antiserum against VR-Pvs230 was generated by DNA immunization. Western blot analyses revealed that mouse anti-Pvs230 serum recognized a high molecular weight band (>250 kDa) in *P. vivax* gametocyte-enriched samples under non-reducing condition (Fig. 2A, lane anti-Pvs230). There was no reactivity of antiserum produced with empty plasmid (Fig. 2A, lane anti-VR1020).

IFA was performed to determine the localization of Pvs230 in the parasite. In fluorescent microscopy, mouse anti-Pvs230 serum specifically reacted with the *P. vivax* gametocyte (Fig. 2B, top panels). In contrast, asexual blood-stage parasites and uninfected erythrocytes did not show any fluorescent signal other than the DAPI nuclear staining (Fig. 2B, top panels). Control serum (VR1020) did not show any reactivity on the parasites and uninfected erythrocytes (Fig. 2B, middle panels). To confirm the localization of Pvs230, the IFA slide was also observed by confocal microscopy. Fluorescence signal was localized on the outer most regions of gametocyte (Fig. 2B, bottom panels) suggesting that Pvs230 might be a surface protein of gametocytes; however further studies involving staining of live parasite is required to confirm the same.

3.2. Anti-Pvs230 antibody inhibits transmission of P. vivax sample collected from the patient

To evaluate whether mouse anti-Pvs230 serum blocks *P. vivax* transmission to the vector mosquitoes, the transmission-blocking assay was carried out using three *P. vivax* samples collected from three independent Thai patients singly infected with *P. vivax* (Table 1). The results showed that the anti-Pvs230 serum significantly reduced the number of oocysts per midgut formed by all the three *P. vivax* samples both in the presence and absence of complement (Table 1) when compared to the anti-VR1020 serum (control). Moreover, the antiserum significantly reduced the oocyst infection rate when the mosquitoes were fed with sample #1 (with or without complement), and sample #3 (in the absence of complement) (Table 1).

3.3. Limited polymorphism in Pvs230 CRDs I–IV

In order to prevent the parasites from evading the immunity induced by vaccines, it is critical to design a vaccine based on protein sequences with minimum polymorphisms. To analyze the extent of polymorphism (i.e., amino acid substitutions) in the DNA vaccine target region (i.e., aa 236–943) of Pvs230 proteins of all the three Thai parasite samples used in our membrane feeding assay, we sequenced region of *Pvs230* encoding aa 236–943 in all the three parasite samples. Among the three parasite specimens, two of them (#2 and #3) had identical amino acid substitutions (i.e., V236F and T743D) as we had reported previously [17]. The sample #1 showed a new amino acid substitution at A484T in addition to V236F and T743D (Fig. 3).

4. Discussion

We have demonstrated that a plasmid VR-Pvs230 encoding CRDs I–IV (aa 236–943) of Pvs230 (Fig. 1A) successfully induced the production of mouse antibody that can recognize native Pvs230 protein on the parasite, and significantly reduce the number of oocysts in the mosquito midgut and hence interfere the transmission of *P. vivax* to humans through mosquitoes. This is the first study that demonstrates the expression of Pvs230 protein in the vivax parasite and the transmission-blocking efficacy of anti-Pvs230 serum on *P. vivax*. Despite the fact that VR-Pvs230 was generated from the sequence of *P. vivax* Sal-1 originated from Central America [21], the mouse antibody against VR-Pvs230 efficiently recognized the parasite isolated in Thailand and also reduced its transmission.

A previous study showed that the antibody raised against an *E. coli* expressed N-terminal fragment of Pfs230 denoted as r230/MBP.C [i.e., aa 443–1132, covering upstream pro-domain and CRDs I–III) (Fig. 1B) that is fused with maltose-binding protein (MBP)] recognized the surface of gametes, and reduced the infectivity of *P. falciparum* to mosquitoes in the presence of complement [16]. This was the first demonstration of the transmission-blocking activity by antibody against a recombinant Pfs230 antigen. Therefore, we designed the construct VR-Pvs230 encoding CRDs I–IV of Pvs230 in this study as an initial attempt (Fig. 1A). Since there is no conservation between the pro-domains of Pfs230 and Pvs230 based on the alignment of the deduced amino acid sequences of Pfs230 and Pvs230 [17], we did not incorporate the pro-domain of Pvs230 in our construct.

In a previous report, all of the transmission-blocking monoclonal antibodies against Pfs230 recognized conformational epitopes on the parasite antigen [22]. Owing to the presence of cysteine rich sequences in Pfs230, Pfs230 forms a complicated tertiary structure [15]. This fact indicates that the creation of properly folded conformation of the epitopes of the TBV candidate is critical for the success of transmission-blocking activity. Previously, DNA immunization with a mammalian expression system (Vical plasmid VR1020) was able to generate strong transmission-blocking antibodies for Pfs25 [23], and Pvs25 [24]. A DNA vaccination using a plasmid expressing Pfs230 region C (aa 443–1132) was tried in an attempt to obtain a higher TBA activity than that can be obtained with vaccination using *E. coli*-expressed recombinant protein, r230/MBP.C [25]. Though the antibody titers induced by the Pfs230 region C DNA immunization in mice were measurable, they failed to block transmission [25]. In this study, DNA vaccine (VR-Pvs230) encoding Pvs230 CRDs I–IV was able to induce antibody that recognizes parasite-produced Pvs230 by western blot analysis under non-reducing condition and by IFA, suggesting that the Pvs230 proteins expressed by the DNA vaccine posses at least in part properly folded conformational epitopes. Importantly, anti-Pvs230 antibody raised against the DNA vaccine reduced the oocyst number in the mosquito and interestingly, the reduction was observed both in the presence and absence of active complement (Table 1). The antiserum also reduced the oocyst infection rate when the mosquitoes were fed with sample #1, and with sample #3 (Table 1), however the efficacy measured by the oocyst infection rate appears lower than those measured by oocyst number. Moreover, in sample #2, oocyst number was significantly reduced, but not the oocyst infection rate. These differences are consistent with our recent findings of Pfs230 TBV [12], suggesting that a higher titer of antibody may be required to make oocyst infection rate zero and achieve complete transmission-blocking. The reason for the transmission-blocking activity even in the absence of active complement may be due to the presence of antibody, in the antiserum, that block biological function such as blocking of the fertilization of gametes besides the antibody that is involved in the complement-mediated lysis of gametes. Another possibility

	Amino acid positions						
	236	237	238	300	488	743	898
Sal-1 (reference)	V	V	A	L	A	T	S
Thai parasite sample #1	F				T	D	
Thai parasite sample #2	F				A	D	
Thai parasite sample #3	F				A	D	
Previous study on Thai samples [ref. 17]	F	M	D	I/V		D	N

Fig. 3. Analysis of polymorphism in the region of Pvs230 targeted by DNA vaccine "VR-Pvs230". Nonsynonymous SNP sites in the domain I through IV (encompassing aa 236–943) of Pvs230 proteins of all the three Thai parasite samples used in our membrane feeding assay were analyzed. The numbers refer to the position of amino acids in Pvs230 protein of Sal-1 strain. Only the amino acid substitution sites were indicated. The polymorphism data in Thai vivax samples reported from our previous study [17] was also used for the comparative analysis. Amino acid substitutions found in Thailand were shaded in gray. A newly found substitution site was indicated at amino acid position 484.

Table 1
Transmission-blocking effects of the mouse antisera produced by DNA immunization on the parasite specimen from *Plasmodium vivax* cases.

P. vivax sample[a]	Plasmids	Heat inactivation[b]	Oocyst numberMedian (IQR[c])	P[d]	Infection rate(Inf/Diss[e])		P[f]
#1	VR1020	Yes	6.0 (1.75–8.0)		85%	17/20	
	VR-Pvs230	Yes	0 (0–0)	<0.0001	10%	2/20	0.0039
	VR1020	No	9.0 (6.75–10.0)		95%	19/20	
	VR-Pvs230	No	0 (0–0.25)	<0.0001	25%	5/20	0.0334
#2	VR1020	Yes	3.5 (1.0–12.25)		90%	18/20	
	VR-Pvs230	Yes	2.0 (0–4.0)	0.0436	65%	13/20	0.6321
	VR1020	No	3.5 (0–8.25)		70%	14/20	
	VR-Pvs230	No	0 (0–1.25)	0.0118	45%	9/20	0.4424
#3	VR1020	Yes	4.0 (2.0–7.0)		90%	18/20	
	VR-Pvs230	Yes	0 (0–0)	<0.0001	20%	4/20	0.0161
	VR1020	No	4.0 (1.75–6.25)		80%	16/20	
	VR-Pvs230	No	0 (0–0.25)	<0.0001	25%	5/20	0.0593

[a] Membrane feeding assay was carried out using isolates obtained from three Thai patients singly infected with *P. vivax*.
[b] Heat-inactivated mouse antisera was diluted with unheated (complement plus) or heat-inactivated (complement minus) AB+ human serum from malaria naïve Thai volunteers in the ratio of 1:1.
[c] IQR; inter-quartile range.
[d] For comparing the transmission-blocking effect of Pvs230 immune mouse serum with the matched VR1020-immune mouse serum, the median number of oocyst was statistically analyzed (Mann–Whitney *U* test) and *P*-values less than 0.05 were considered statistically significant.
[e] The oocyst prevalence was calculated by number of oocyst-infected mosquitoes per 20 mosquitoes dissected in each group (Inf/Diss).
[f] Difference between the transmission-blocking effect of Pvs230 and VR1020 immune serum groups was statistically analyzed by Fisher's exact test. *P*-values less than 0.05 were considered statistically significant.

is that the use of Vaxfectin® as adjuvant might have enhanced the titer of Pvs230-specific antibody, for the intramuscular injection of Vaxfectin® formulated with a plasmid DNA encoding influenza nucleoprotein increased antibody titers up to 20-fold, to levels that could not be reached with the plasmid DNA alone [19]. However to validate this claim, we need further studies involving the measurement of antibody titer using properly folded recombinant Pvs230 protein as capture antigen.

In our recent report on the polymorphism of Pvs230, we found 10 amino acid substitutions within the CRDs I–IV (aa 236–943) among isolates worldwide[17]. Six out of 10 amino acid substitutions in comparison with Sal-1 sequence were found in the Thai isolates used in the previous study ($n = 20$) [17] (Fig. 3). Among the three parasite specimens used in our membrane feeding assay, two of them (#2 and #3) had identical amino acid substitutions (i.e., V236F and T743D) in the target region (i.e., aa 236–943) of Pvs230. The sample #1 showed a new amino acid substitution at A484T in addition to V236F and T743D (Fig. 3). This analysis shows that the polymorphism in Pvs230 is limited and it may not pose a problem for the utilization of Pvs230 CRDs I–IV as an effective TBV candidate. Further study using larger number of vivax cases is necessary to confirm this preliminary observation about the effect of polymorphism on TBV efficacy.

Acknowledgments

We thank the staff of the Department of Entomology, Armed Forces Research Institute of Medical Sciences, Bangkok, Thailand, for their technical assistance, and Thangavelu U. Arumugam for the critical reading of the manuscript. We also thank Vical Inc. for providing the VR1020 DNA vaccine plasmid and Vaxfectin® adjuvant. This research was supported in part by the Ministry of Education, Culture, Sports, Science and Technology (21022034, 21249028, 21406010, 23406007), and by the Ministry of Health, Labour, and Welfare, Japan (H21-Chikyukibo-ippan-005).

References

[1] WHO. World Malaria Report 2010. Geneva, Switzerland: WHO Press; 2010.
[2] Price RN, Tjitra E, Guerra CA, Yeung S, White NJ, Anstey NM. Vivax malaria: neglected and not benign. Am J Trop Med Hyg 2007;77:79–87.
[3] Mueller I, Galinski MR, Baird JK, Carlton JM, Kochar DK, Alonso PL, et al. Key gaps in the knowledge of *Plasmodium vivax*, a neglected human malaria parasite. Lancet Infect Dis 2009;9:555–66.
[4] Kaneko A, Taleo G, Kalkoa M, Yamar S, Kobayakawa T, Bjorkman A. Malaria eradication on islands. Lancet 2000;356:1560–4.
[5] Arevalo-Herrera M, Chitnis C, Herrera S. Current status of *Plasmodium vivax* vaccine. Hum Vaccin 2010;6:124–32.
[6] Herrera S, Bonelo A, Perlaza BL, Fernandez OL, Victoria L, Lenis AM, et al. Safety and elicitation of humoral and cellular responses in Colombian malaria-naive volunteers by a *Plasmodium vivax* circumsporozoite protein-derived synthetic vaccine. Am J Trop Med Hyg 2005;73:3–9.
[7] Malkin EM, Durbin AP, Diemert DJ, Sattabongkot J, Wu Y, Miura K, et al. Phase 1 vaccine trial of Pvs25H: a transmission blocking vaccine for *Plasmodium vivax* malaria. Vaccine 2005;23:3131–8.
[8] Wu Y, Ellis RD, Shaffer D, Fontes E, Malkin EM, Mahanty S, et al. Phase 1 trial of malaria transmission blocking vaccine candidates Pfs25 and Pvs25 formulated with Montanide ISA 51. PLoS ONE 2008;3:e2636.
[9] Kaslow DC, Quakyi IA, Syin C, Raum MG, Keister DB, Coligan JE, et al. A vaccine candidate from the sexual stage of human malaria that contains EGF-like domains. Nature 1988;333:74–6.
[10] Tsuboi T, Kaslow DC, Gozar MM, Tachibana M, Cao YM, Torii M. Sequence polymorphism in two novel *Plasmodium vivax* ookinete surface proteins, Pvs25 and Pvs28, that are malaria transmission-blocking vaccine candidates. Mol Med 1998;4:772–82.
[11] Williamson KC, Criscio MD, Kaslow DC. Cloning and expression of the gene for *Plasmodium falciparum* transmission-blocking target antigen, Pfs230. Mol Biochem Parasitol 1993;58:355–8.
[12] Tachibana M, Wu Y, Iriko H, Muratova O, MacDonald NJ, Sattabongkot J, et al. N-terminal prodomain of Pfs230 synthesized using a cell-free system is sufficient to induce complement-dependent malaria transmission-blocking activity. Clin Vaccine Immunol 2011;18:1343–50.
[13] van Dijk MR, van Schaijk BC, Khan SM, van Dooren MW, Ramesar J, Kaczanowski S, et al. Three members of the 6-cys protein family of *Plasmodium* play a role in gamete fertility. PLoS Pathog 2010;6:e1000853.
[14] Carter R, Coulson A, Bhatti S, Taylor BJ, Elliott JF. Predicted disulfide-bonded structures for three uniquely related proteins of *Plasmodium falciparum*, Pfs230, Pfs48/45 and Pf12. Mol Biochem Parasitol 1995;71:203–10.
[15] Gerloff DL, Creasey A, Maslau S, Carter R. Structural models for the protein family characterized by gamete surface protein Pfs230 of *Plasmodium falciparum*. Proc Natl Acad Sci U S A 2005;102:13598–603.
[16] Williamson KC, Keister DB, Muratova O, Kaslow DC. Recombinant Pfs230, a *Plasmodium falciparum* gametocyte protein, induces antisera that reduce the infectivity of *Plasmodium falciparum* to mosquitoes. Mol Biochem Parasitol 1995;75:33–42.
[17] Doi M, Tanabe K, Tachibana S, Hamai M, Tachibana M, Mita T, et al. Worldwide sequence conservation of transmission-blocking vaccine candidate Pvs230 in *Plasmodium vivax*. Vaccine 2011;29:4308–15.
[18] Han ET, Watanabe R, Sattabongkot J, Khuntirat B, Sirichaisinthop J, Iriko H, et al. Detection of four *Plasmodium* species by genus- and species-specific loop-mediated isothermal amplification for clinical diagnosis. J Clin Microbiol 2007;45:2521–8.
[19] Hartikka J, Bozoukova V, Ferrari M, Sukhu L, Enas J, Sawdey M, et al. Vaxfectin enhances the humoral immune response to plasmid DNA-encoded antigens. Vaccine 2001;19:1911–23.
[20] Sullivan SM, Doukas J, Hartikka J, Smith L, Rolland A. Vaxfectin: a versatile adjuvant for plasmid DNA- and protein-based vaccines. Expert Opin Drug Deliv 2010;7:1433–46.
[21] Collins WE, Contacos PG, Krotoski WA, Howard WA. Transmission of four Central American strains of *Plasmodium vivax* from monkey to man. J Parasitol 1972;58:332–5.

[22] Read D, Lensen AH, Begarnie S, Haley S, Raza A, Carter R. Transmission-blocking antibodies against multiple, non-variant target epitopes of the *Plasmodium falciparum* gamete surface antigen Pfs230 are all complement-fixing. Parasite Immunol 1994;16:511–9.
[23] Lobo CA, Dhar R, Kumar N. Immunization of mice with DNA-based Pfs25 elicits potent malaria transmission-blocking antibodies. Infect Immun 1999;67:1688–93.
[24] Kongkasuriyachai D, Bartels-Andrews L, Stowers A, Collins WE, Sullivan J, Sattabongkot J, et al. Potent immunogenicity of DNA vaccines encoding *Plasmodium vivax* transmission-blocking vaccine candidates Pvs25 and Pvs28-evaluation of homologous and heterologous antigen-delivery prime-boost strategy. Vaccine 2004;22:3205–13.
[25] Fanning SL, Czesny B, Sedegah M, Carucci DJ, van Gemert GJ, Eling W, et al. A glycosylphosphatidylinositol anchor signal sequence enhances the immunogenicity of a DNA vaccine encoding *Plasmodium falciparum* sexual-stage antigen, Pfs230. Vaccine 2003;21:3228–35.

Vaccine 30 (2012) 1972–1980

Contents lists available at SciVerse ScienceDirect

Vaccine

journal homepage: www.elsevier.com/locate/vaccine

Antibodies against a *Plasmodium falciparum* antigen PfMSPDBL1 inhibit merozoite invasion into human erythrocytes

Hirokazu Sakamoto[a], Satoru Takeo[a], Alexander G. Maier[c,1], Jetsumon Sattabongkot[d,2], Alan F. Cowman[c], Takafumi Tsuboi[a,b,e,*]

[a] *Cell-Free Science and Technology Research Center and Ehime University, Matsuyama, Ehime 790-8577, Japan*
[b] *Venture Business Laboratory, Ehime University, Matsuyama, Ehime 790-8577, Japan*
[c] *The Walter and Eliza Hall Institute for Medical Research, Melbourne, Victoria 3052, Australia*
[d] *Department of Entomology, Armed Forces Research Institute of Medical Sciences, Bangkok 10400, Thailand*
[e] *Ehime Proteo-Medicine Research Center, Ehime University, Toon, Ehime 791-0295, Japan*

ARTICLE INFO

Article history:
Received 11 October 2011
Received in revised form 4 January 2012
Accepted 5 January 2012
Available online 14 January 2012

Keywords:
Blood-stage vaccine
Merozoite
Malaria
PfMSPDBL1
Plasmodium falciparum

ABSTRACT

One approach to develop a malaria blood-stage vaccine is to target proteins that play critical roles in the erythrocyte invasion of merozoites. The merozoite surface proteins (MSPs) and the erythrocyte-binding antigens (EBAs) are considered promising vaccine candidates, for they are known to play important roles in erythrocyte invasion and are exposed to host immune system. Here we focused on a *Plasmodium falciparum* antigen, PfMSPDBL1 (encoded by PF10_0348 gene) that is a member of the MSP3 family and has both Duffy binding-like (DBL) domain and secreted polymorphic antigen associated with merozoites (SPAM) domain. Therefore, we aimed to characterize PfMSPDBL1 as a vaccine candidate. Recombinant full-length protein (rFL) of PfMSPDBL1 was synthesized by a wheat germ cell-free system, and rabbit antiserum was raised against rFL. We show that rabbit anti-PfMSPDBL1 antibodies inhibited erythrocyte invasion of wild type parasites *in vitro* in a dose dependent manner, and the specificity of inhibitory activity was confirmed using PfMSPDBL1 knockout parasites. Pre-incubation of the anti-PfMSPDBL1 antibodies with the recombinant SPAM domain had no effect on the inhibitory activity suggesting that antibodies to this region were not involved. In addition, antibodies to rFL were elicited by *P. falciparum* infection in malaria endemic area, suggesting the PfMSLDBL1 is immunogenic to humans. Our results suggest that PfMSPDBL1 is a novel blood-stage malaria vaccine candidate.

1. Introduction

Malaria is a serious infectious disease caused by a protozoan parasite of the genus *Plasmodium*. It causes approximately 300 million illnesses and 1 million deaths annually [1]. The appearance of malaria parasites with resistance to antimalarial drugs and of mosquito vector with resistance to insecticides has highlighted the importance of developing a malaria vaccine. Protective immunity against *Plasmodium falciparum* develops after repeated exposure and prevents severe disease and symptomatic episodes by controlling blood-stage parasitemia [2]. Antibodies are important effectors of protective immunity against malaria as evidenced by experimental animal models and, most importantly, passive transfer studies in which antibodies from malaria-immune adults were successfully used to treat patients with severe malaria [3,4]. These findings provide a strong rationale that an effective vaccine is achievable against the asexual blood-stage parasites by inducing an immune response. Although a number of blood-stage vaccines have been developed and tested in preclinical and clinical trials, only limited clinical success has been achieved with blood-stage vaccines to date [5,6]. Therefore, discovery of novel blood-stage vaccine candidates is an important step towards control of malaria.

One approach to discover a novel malaria vaccine candidate is to target proteins that play critical roles in the invasion process into erythrocytes. The invasion involves multiple steps, including initial attachment, apical reorientation, and tight junction formation, followed by the entry of the merozoite into the erythrocyte. The initial attachment between a free merozoite and an erythrocyte is a reversible interaction and thought to be mediated by merozoite surface proteins (MSPs) [7]. On the other hand, the tight junction formation requires the function of erythrocyte-binding

* Corresponding author at: Cell-Free Science and Technology Research Center, Ehime University, Matsuyama, Ehime 790-8577, Japan. Tel.: +81 89 927 8277; fax: +81 89 927 9941.
E-mail address: tsuboi@ccr.ehime-u.ac.jp (T. Tsuboi).
[1] Present address: Department of Biochemistry, La Trobe Institute for Molecular Science, La Trobe University, Melbourne, Victoria 3086, Australia.
[2] Present address: Mahidol Vivax Research Center, Faculty of Tropical Medicine, Mahidol University, Bangkok, Thailand.

0264-410X/$ – see front matter © 2012 Elsevier Ltd. All rights reserved.
doi:10.1016/j.vaccine.2012.01.010

antigens (EBAs). The EBAs are members of the Duffy binding-like (DBL) superfamily, EBA175 (encoded by MAL7P1.176 gene), EBA140/BAEBL (by MAL13P1.160 gene) and EBA181/JESEBL (by PFA0125c gene) are expressed within *P. falciparum* [8]. The EBAs are stored in the micronemes and are secreted onto the merozoite surface just before invasion, and serve as ligands that bind to receptors on the surface of erythrocytes [9–11]. A number of studies have shown that antibodies to these merozoite antigens are thought to function *in vivo* by inhibiting merozoite invasion of erythrocyte (ligand-blocking), opsonizing merozoites for phagocytosis, and inducing antibody-dependent cellular inhibition (ADCI) [12–15]. Since the MSPs and EBAs are exposed to the host immune system, these proteins are considered as promising vaccine candidates and some of these are at various stages of development for clinical trials [16].

Here, we have focused on a novel antigen PfMSPDBL1 (encoded by PF10_0348 gene). This protein has a DBL domain and secreted polymorphic antigen associated with merozoites (SPAM) (Fig. 1A). A previous report [17] showed that the PfMSPDBL1 protein is localized on the merozoite surface and it can bind to the erythrocytes and hence suggested that PfMSPDBL1 may play a role in initial attachment of the erythrocyte by merozoites and that the DBL domain may be a potential target of ligand-blocking antibodies as well as DBL domains of other erythrocyte binding proteins. However, there were not any assays performed in the previous study to prove the invasion inhibitory effect of the anti-PfMSPDBL1 antibodies [17]. On the other hand, recently, a new MSP3 multi-gene family was predicted, and PfMSPDBL1 is one of the members of this family [18]. Because of the high conservation of the MSP3-family in the SPAM domain, antibody against one member cross-reacted to the other MSP3 family members. Importantly, these "cross-reactive" human antibodies inhibited parasite growth in antibody dependent cellular inhibition (ADCI) assays [18]. However, the inhibition was attributed to the "cross-reactive" antibodies, so it is still not known if antibodies that specifically bind to PfMSPDBL1 contributed to this inhibition. In this study, we have investigated the effects of specific antibodies against PfMSPDBL1 protein on erythrocyte invasion by merozoites using growth inhibition assays.

2. Materials and methods

2.1. Recombinant plasmid construction for protein expression

All recombinant plasmids were constructed using pEU plasmids that are designed specifically for the wheat germ cell-free protein expression system (CellFree Sciences, Matsuyama, Japan) [19]. The nucleotide sequence of the cloned inserts were confirmed using ABI PRISM® 3100-Avant Genetic Analyzer (Applied Biosystems, Foster City, CA). A gene encoding full length [FL, amino acid positions (aa) 26–697] without N-terminal signal peptide of the PfMSPDBL1 (Fig. 1A) and a gene fragment encoding $PfMSP1_{19}$ (aa 1607–1688) were amplified by PCR from the cDNA of *P. falciparum* 3D7 strain. The FL of PfMSPDBL1 gene was cloned into pEU-E01-His-(TEV)-N2 vector between *Xho* I and *Not* I sites (shown in small letters in the primer sequences below), and $PfMSP1_{19}$ gene were cloned into pEU-E01-GST-(TEV)-N2 vector between *Xho* I and *Not* I sites. The nucleotide sequences of the primer pairs used in the PCR amplification were as follows: FL_0076F (5′-ctcgagAATGACCTAATAAATTATAATGATTCGAATCTAAGAAACG-3′), FL_2091R (5′-gcggccgcCTATTTTTGAAATAAATCTGTCATATCTTCTG-TCAAACC-3′), msp1-19F (5′-ctcgagATGAACATTTCACAACACCAAT-GC-3′), msp1-19R (5′-gcggccgcTCAACTGCAGAAAATACCATCGA-3′). To prevent a slippage of RNA polymerase at AT-rich region of *pfmspdbl1* gene and hence potential frame-shift during transcription step, codon optimization was performed using PrimeSTAR® Mutagenesis Basal Kit (Takara, Otsu, Japan) at three regions of adenine-repeat sequences for the FL construct (Fig. 1B). The primer sequences used in the PCR amplifications were as follows: 701–707 bp_F (5′-TAAAG*A*G*AA*G*AA*TCTGAATGCCCTTACAGC-3′), 701–707 bp_R (5′-CAGA*TT*C*TT*C*T*CTTTATAATGTTTCATTAAAGC-3′), 1363–1370 bp_F (5′-TAAC*AA*G*AA*G*AA*TCAAGATTCTCTAACAACC-3′), 1363–1370 bp_R (5′-TGA*TT*C*TT*C*TT*GTTATCAATTACTGCTTTAAG-3′), 1871–1875/1901–1909 bp_F (5′-GTG*A*G*AA*G*AA*G*A*GTA-TTTCAAAAGTTGACGAAG-3′), 1871–1875/1901–1909 bp_R (5′-TAC*T*C*TT*C*TT*C*T*CACTTTGTTGTTGATTACTGAGTTC*CTTCT*CCTTA-3′). The italic letters and underlined sequences in the above primers indicate the adenine-repeat sequences and the target bases for codon optimization, respectively. Finally, FL was amplified by PCR from the optimized FL clone, and subcloned into pEU-E01-MCS vector between *Xho* I and *Not* I sites. The primer sequence pair used in the PCR amplification was as follows: FL_atg-0076F (5′-ctcgagATGAATGACCTAATAAATTATAATGATTCGAA-3′), FL_2091R-6His (5′-gcggccgcCTAGTGATGATGATGATGATGTTTTTGAAATAAA-TCTGTCATATCTTCTGTC-3′). The small letters and underlined sequences in the above primers indicate the restriction site of *Xho* I or *Not* I, and hexa-His tag, respectively.

To express SPAM domains of member of MSP3 family [18], six conserved SPAM domains of the MSP3 family members were amplified by PCR from the cDNA of *P. falciparum* 3D7 strain, and cloned into pEU-E01-His-(TEV)-N2 vector between *Xho* I and *Not* I sites. The primer sequence pairs used in the PCR amplification were as follows: MSP3.1_0499F (5′-ctcgagTATGAAAAGGCAAAAAATGCT-3′), MSP3.1_1065R (5′-gcggccgcTTAATGATTTTTAAAATATTTGGA-3′), MSP3.2_0481F (5′-ctcgagTCTGAAACAAATAAAAATCCTACTTCTCAT-3′), MSP3.2_1116R (5′-gcggccgcTTAATTATTACTAAATAGATGGATCATTTCTTG-3′), MSP3.3_0682F (5′-ctcgagTATGAGAAGAAAAATGAAAATA-3′), MSP3.3_1275R (5′-gcggccgcTTAATTATATGTAAAAAATTCCAT-3′), MSP3.4_1522F (5′-ctcgagGATAATGTAAACTCTGTAACG-3′), MSP3.4_2094R (5′-gcggccgcTTATTTTTGAAATAAATCTGTCAT-3′), MSP3.7_0640F (5′-ctcgagCCTGAAGGACCAAGAGCAAA-3′), MSP3.7_1218R (5′-gcggccgcTCAATAGTTATTTAAAAAAAAAGT-3′), MSP3.8_1609F (5′-ctcgagCATGAAAGTAATGTTGGTAG-3′), MSP3.8_2289R (5′-gcggccgcTTAATTTTTAAATAAATTTGTAAT-3′). The small letters in the above primers indicate the restriction site of *Xho* I or *Not* I.

2.2. Production of recombinant proteins and antibodies

We employed the wheat germ cell-free protein expression system (CellFree Sciences) and synthesized recombinant proteins as described previously [20–23]. The recombinant FL protein encompassing the DBL and SPAM domains encoded by amino acids 26–697 was cloned as a C-terminal His-tagged protein (rFL; Fig. 1A) and the six SPAM domains of the MSP3 family members [18] were cloned as N-terminal His-tagged proteins. These proteins were synthesized and purified using Ni-Sepharose column (GE Healthcare, Camarillo, CA). The GST-fused $PfMSP1_{19}$ was captured using Glutathione-Sepharose 4B column (GE Healthcare), and subsequently $PfMSP1_{19}$ was eluted by on-column cleavage with 60 U of AcTEV protease (Invitrogen).

To generate antibodies against rFL, one Japanese white rabbit was immunized subcutaneously with 250 μg of purified proteins with Freund's complete adjuvant, followed by 250 μg with Freund's incomplete adjuvant thereafter. To generate antibodies against $PfMSP1_{19}$, two BALB/c mice were immunized subcutaneously with 30 μg of purified proteins per mouse with Freund's complete adjuvant, followed by 30 μg with Freund's incomplete adjuvant thereafter. All immunizations were done 3 times at 3-week intervals. The antisera were collected 14 days after the last immunization. All animal experimental protocols were approved

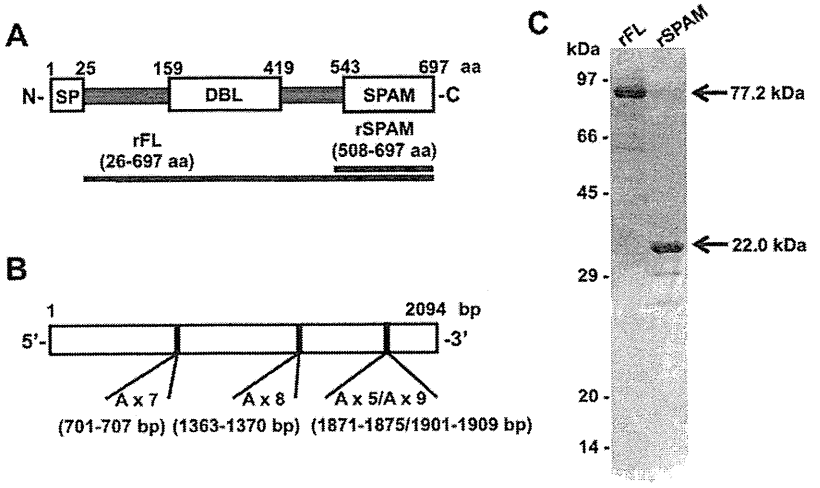

Fig. 1. PfMSPDBL1 primary structure, design of constructs, recombinant proteins. (A) Schematic representation of the primary structure of PfMSPDBL1 showing signal peptide (SP, amino acid (aa) 1–25), Duffy binding-like (DBL, aa 159–419) domain and secreted polymorphic antigen associated with merozoites (SPAM, aa 543–697) domain. The black bars highlight the region of the expressed recombinant proteins (rFL, aa 26–697; rSPAM, aa 508–697). (B) The three vertical lines show the codon optimized adenine-rich sites; 7 consecutive adenines, 701–707 bp; 8 consecutive adenines, 1363–1370 bp; 5 and 9 consecutive adenines, 1871–1875 bp and 1901–1909 bp, respectively. The consecutive adenines in these sites were synonymously substituted to guanines by site-directed mutagenesis described in Section 2. (C) SDS-PAGE of recombinant proteins. The purified proteins resolved in a SDS-PAGE and stained with Coomassie brilliant blue R-250 are shown. The two black arrows show purified recombinant FL and SPAM proteins. The arrows show the predicted molecular mass of rFL and rSPAM.

by the Institutional Animal Care and Use Committee of Ehime University, and the experiments were conducted according to the Ethical Guidelines for Animal Experiments of Ehime University.

2.3. Parasite culture

The 3D7 strain of *P. falciparum* and the *pfmspdbl1* (PF10_0348) knockout clone of *P. falciparum* (3D7ΔDBL1) (Uboldi et al., in preparation) were maintained in human O+ erythrocytes obtained from the Japanese Red Cross Society as previously described [24]. To harvest parasite pellets, mature schizonts were purified using Percoll (GE Healthcare, Camarillo, CA) density gradient centrifugation and further treated with tetanolysin (List Biological Laboratories, Campbell, CA), washed with phosphate buffered saline (PBS) containing "Complete Protease Inhibitor" (Roche, Mannheim, Germany) and stored at −80 °C until used.

2.4. Preparation of the cDNA

Total RNA was extracted from 3D7 parasite-infected erythrocytes rich in schizonts, using Trizol (Invitrogen, Carlsbad, CA) as recommended by the manufacturers and treated with DNase1 (Invitrogen) at 37 °C for 15 min. Superscript III® was used to reverse transcribe DNA-free RNA primed with random hexamer primers (Invitrogen) at 25 °C for 10 min followed by at 50 °C for 50 min and at 85 °C for 5 min.

2.5. Western blot analysis

P. falciparum native proteins from both 3D7 and 3D7ΔDBL1 parasites rich in schizont were extracted in SDS-PAGE loading buffer and subjected to electrophoresis (1×10^6 infected erythrocytes/lane) under reducing condition on a 12.5% polyacrylamide gel (ATTO, Tokyo, Japan). Proteins were transferred to a 0.2 μm PVDF membrane (BioRad, Hercules, CA). After transfer, the membrane was blocked with 5% non-fat milk/PBST (1× PBS/0.1% tween20) at room temperature (RT) for 1 h and probed with anti-rFL serum diluted (1:1000) in PBST. After washing the membrane with PBST, it was incubated with horseradish peroxidase (HRP) conjugated secondary antibodies (GE Healthcare) at RT for 30 min, followed by visualization with Immobilon™ Western Chemiluminescent HRP Substrate (Millipore, Billerica, MA) on LAS 4000 mini luminescent image analyzer (GE Healthcare). The relative molecular sizes of the proteins were calculated with reference to molecular weight size marker "magic mark XP" (Invitrogen).

For cross-reactivity testing for the SPAM domains from MSP3 family members (Fig. 2C), the proteins (100 ng/lane) were subjected to electrophoresis under reducing condition on a 12.5% polyacrylamide gel (ATTO). Western blot analysis was performed as described above. Anti-penta His monoclonal antibody (Qiagen), anti-rFL serum and pooled human sera were used as primary antibodies at 1:500 dilution. The pooled human sera include five individual sera, and a detailed explanation for human sera is given in ELISA section.

2.6. Indirect immunofluorescence assay (IFA)

Thin smears of schizont-enriched *P. falciparum* (3D7)-infected erythrocytes were prepared on glass slides and stored at −80 °C. The smears were thawed and fixed with 4% formaldehyde in PBS at RT for 15 min and permeabilized with PBS containing 0.1% Triton X-100 (Nacalai Tesque) at RT for 15 min. The smears were blocked with 5% non-fat milk in PBS at 37 °C for 30 min. They were incubated with primary antibodies [both mouse anti-PfMSP1$_{19}$ serum (1:250 dilution) and rabbit anti-rFL serum (1:500 dilution) antibodies] at 37 °C for 1 h. After washing with PBS, slides were incubated at 37 °C for 30 min with Alexa488-conjugated goat anti-rabbit IgG (Invitrogen; 1:500 dilution), Alexa546-conjugated goat anti-mouse IgG (Invitrogen; 1:500 dilution), and 4′,6-diamidino-2-phenylindole HCl (DAPI, 1 μg/ml; Wako Pure Chemical, Osaka, Japan). The slides were mounted in ProLong Gold antifade reagent (Invitrogen) and examined with LSM710 confocal scanning laser microscope (Carl Zeiss MicroImaging, Thornwood, NY). Images were processed with ImageJ software (National Institutes of Health, Rockville, MD).

2.7. Growth inhibition assay

Total IgG to be tested in growth inhibition assays (GIA) was purified from each rabbit antiserum using protein G column (Pierce Inc., Rockford, IL); the purified IgG were dialyzed against RPMI 1640

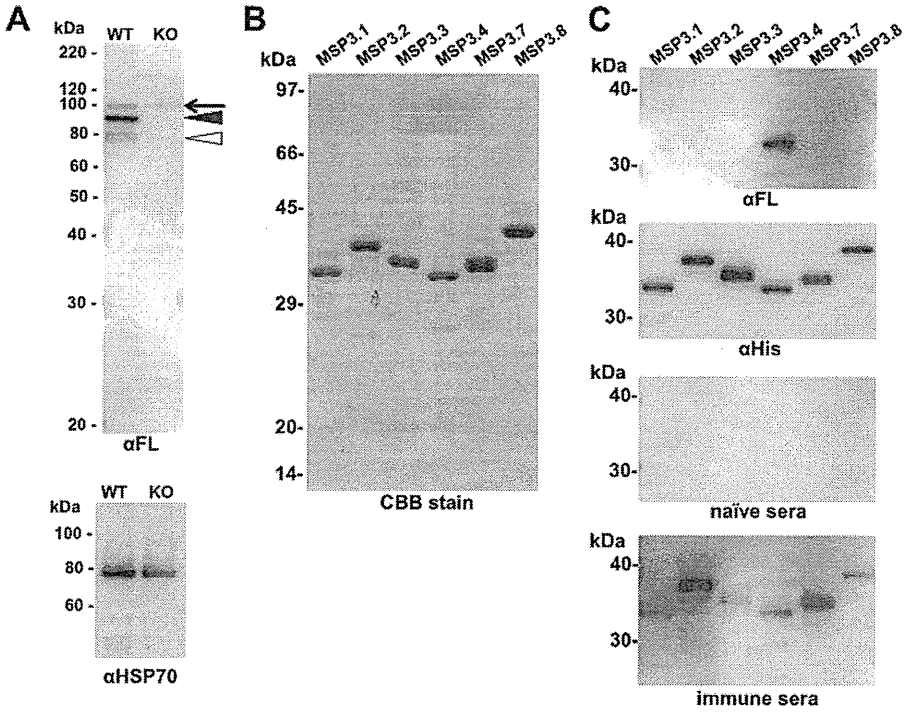

Fig. 2. Anti-PfMSPDBL1 antibodies react to native PfMSPDBL1, but not cross-react to SPAM domains of the other MSP3 family members. (A) Western blot analysis of synchronized schizont lysates of 3D7 (WT) and 3D7ΔDBL1 (KO) probed with the anti-rFL polyclonal antiserum (1:1000 dilution) and the anti-PfHSP70 monoclonal antibody (4C9, 1:500 dilution) as a quantitative loading control. The filled arrowhead indicates the full-length form of the native PfMSPDBL1 (95 kDa), the open arrowhead indicates its processed form (80 kDa) and the arrow indicates a nonspecific signal. (B) Recombinant proteins of six conserved SPAM domains of MSP3 family, consisting of MSP3 (MSP3.1), MSP6 (MSP3.2), H101 (MSP3.3), PfMSPDBL1 (MSP3.4), H103 (MSP3.7) and PfMSPDBL2 (MSP3.8) were expressed, and affinity purified. These proteins were separated on 12.5% SDS-PAGE, and stained by Coomassie Brilliant Blue. (C) Western blot analysis of the recombinant SPAM domains probed with anti-rFL serum (top panel), anti-His antibody (second panel), pooled human naïve sera (third panel), or pooled human immune sera (bottom panel).

(Life Technologies, Gaithersburg, MD) and concentrated with an Amicon Ultra-15 30K (Millipore, Billerica, MA) to a concentration of 40 mg/ml or 80 mg/ml. The purified IgGs were reabsorbed with uninfected human O+ erythrocytes (25 μl of RBCs per 1 ml of serum sample) for 1 h at RT with constant rotation to remove any antibodies that specifically binds to human erythrocytes. After reabsorption, IgGs were sterilized by filtration through a 0.22 μm filter (Nalgene Nunc, Rochester, NY) and stored in aliquots at −80 °C.

The growth inhibition assay was performed in a 40 μl culture medium containing human O+ erythrocyte at 1% hematocrit with 0.2–0.4% initial parasitemia in the presence of rabbit IgG in a 96 well half area flat bottom microtiter plate (Corning Incorporated, Corning, NY) at 37 °C for 24–30 h in a humidified, gassed (with 90% N_2, 5% O_2, and 5% CO_2) box. Each IgG was added to a final concentration of 20 mg/ml during setup of the assay, prior to reinvasion. To test the effects of IgGs on growth per se (i.e., for the GIA in Fig. 4C), the IgGs were added to ring stage parasites at 0.2–0.4% initial parasitemia. For the IgG titration growth inhibition assay anti-rFL IgG was added to the well at a final concentration of 0, 1.25, 2.5, 5, 10, or 20 mg/ml. Parasitemia was scored by counting number of infected

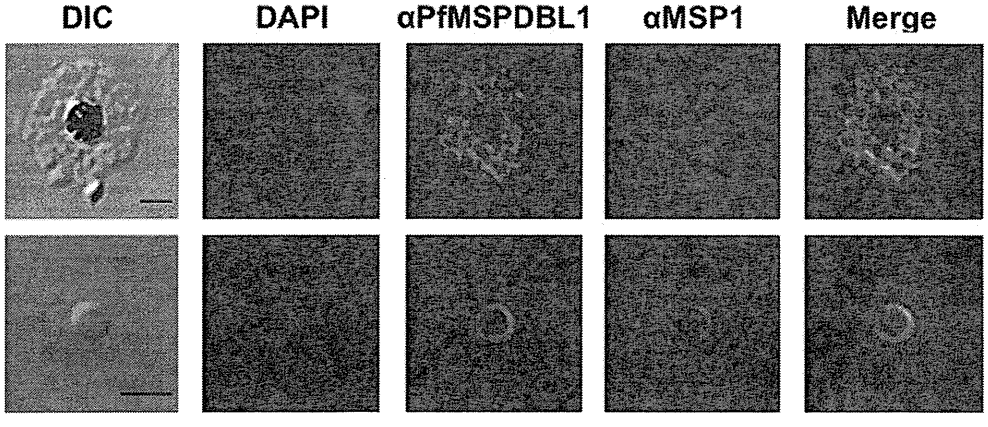

Fig. 3. Native PfMSPDBL1 is localized on the merozoite surface. A mature schizont (Triton X-100 permeabilized; upper panel) and a free merozoite (non-permeabilized; bottom panel) of the 3D7 wild type strain were probed with rabbit anti-rFL serum (green) and mouse anti-MSP1 serum (red). Anti-MSP1 was used as a merozoite surface maker. Parasite nuclei were stained with DAPI (blue). Scale bars represent 2 μm. (For interpretation of the references to color in this figure legend, the reader is referred to the web version of the article.)

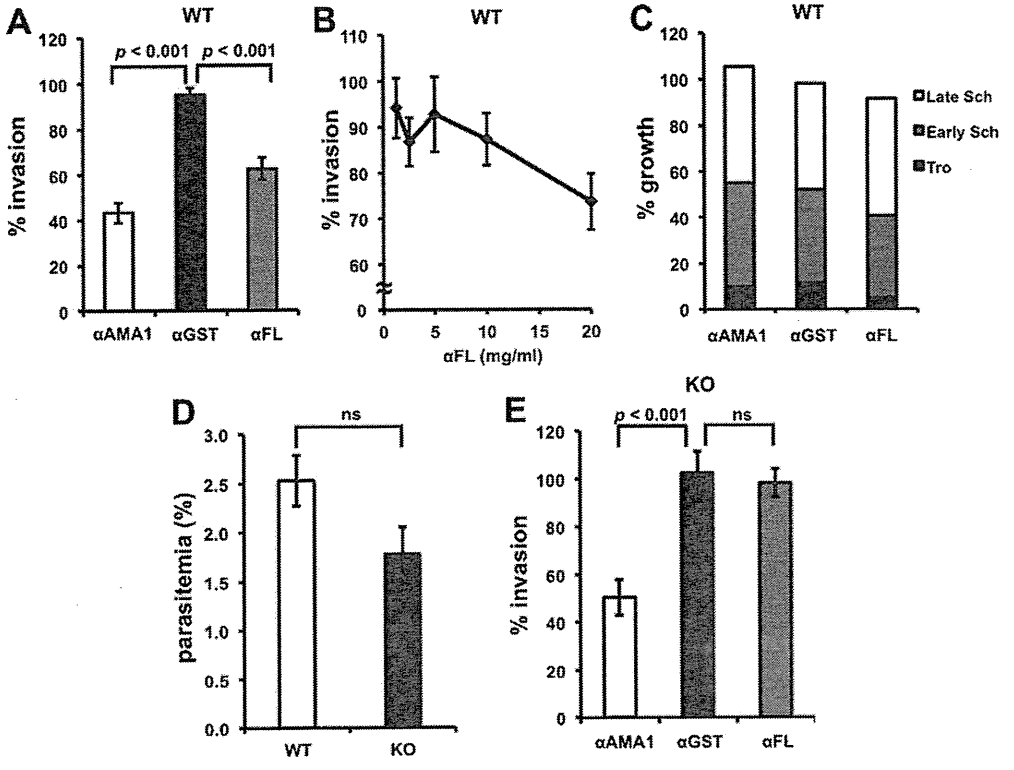

Fig. 4. Anti-PfMSPDBL1 antibodies inhibit erythrocyte invasion of merozoites. (A) Anti-rFL IgG have growth inhibitory activity *in vitro*. The ability of the anti-rFL IgG to inhibit invasion and/or growth was tested in one-cycle growth inhibition assay. Anti-AMA1 and anti-GST IgGs were used as positive and negative controls, respectively. Schizonts of 3D7 wild type strain (at 0.2–0.4% initial parasitemia) were cultured in presence of 20 mg/ml of each IgG. One-way ANOVA was performed ($p < 0.001$) followed by Bonferroni's pairwise multiple comparison tests to compare anti-GST and anti-rFL. (B) Percent invasion of the 3D7 wild type strain in the presence of serially diluted anti-rFL IgG. Final concentrations of the IgG were ranged from 0 to 20 mg/ml. (C) Anti-rFL IgG did not affect intra-erythrocytic parasite growth. Rings of 3D7 wild type strain (at 0.2–0.4% initial parasitemia) were cultured in presence of 20 mg/ml of each IgG. Total percent growth and percentage of different stages {i.e., trophozoites (black bar), early schizonts (grey bar), and late schizonts (white bar)} were compared among the three groups. (D) Disruption of *pfmspdbl1* gene do not affect parasite invasion. Post-invasion parasitemia (%) for the 3D7 (WT) and 3D7ΔDBL1 (KO) parasites are shown. Synchronized schizonts of both WT and KO parasites were diluted at 0.2–0.4% initial parasitemia, and then % parasitemia was determined after 30 h of culture. Mean % parasitemia of the three independent experiments were statistically analyzed using Student's *t*-test. (E) The anti-rFL IgG do not inhibit invasion of the 3D7ΔDBL1 parasite. The ability of the anti-rFL IgG to inhibit invasion and/or growth was tested for the 3D7ΔDBL1 parasite in the same manner as shown in Fig. 4A. One-way ANOVA was performed followed by Bonferroni's pairwise multiple comparison tests to compare anti-GST and anti-rFL. For all panels, the error bars represent standard error of the mean (SEM) of three independent experiments.

erythrocytes in 7000 erythrocytes in Giemsa stained thin smears. Each observed parasitemia was divided by the mean value of the parasitemia in three smears of control culture without antibody to give the percent invasion or growth value in each assay. Three independent assays were performed in triplicate.

For the IgG neutralization assay (Fig. 5B), the anti-rFL IgG was incubated with either rFL, rSPAM or rGST protein at 37 °C for 1 h and centrifuged at 4000 × *g* for 3 min, then the supernatant was added to the culture of *P. falciparum*. Final concentrations of IgG and recombinant proteins were at 20 mg/ml and 0.2 mg/ml, respectively. For IgG neutralization using increasing concentration of rFL protein (Fig. 5C), rFL protein at final concentration of either 0, 0.025, 0.05, 0.1, or 0.2 mg/ml was incubated with the anti-rFL IgG (final concentration is at 20 mg/ml). Percent invasion at each point was calculated as described above.

2.8. ELISA

All the human serum samples for the determination of antibody against PfMSPDBL1 were collected from adult Thai donors. The serum samples from asymptomatic parasite carriers infected with only *P. falciparum* were collected in the village of Ban Kong Mong Tha, western Thailand with written informed consent [25]. Serum samples were also collected from healthy malaria naïve individuals living in Bangkok, Thailand and used as negative controls. The study was approved by the Ethics Committee of the Thai Ministry of Public Health and the Institutional Review Board of the Walter Reed Army Institute of Research [26]. Measurement of anti-PfMSPDBL1 antibodies in human serum samples was performed according to the standardized ELISA protocol. Briefly, 96-well ELISA plates were coated with 50 ng/well of purified rFL protein at 4 °C overnight in coating buffer (20 mM boric acid, pH 8.9). After the plates were blocked with 2 mg/ml of gelatin in coating buffer, the sera were 1:600 diluted in PBST, added to antigen-coated wells in duplicate, and incubated at 37 °C for 1 h. After washing, the plates were incubated with 1:3000 diluted rabbit anti-human IgG HRP conjugate (DakoCytomation, Glostrup, Denmark) in PBST at 37 °C for 1 h. After washing, the plates were incubated with 0.5 mg/ml azino-bis-3-ethylbenthiazoline-6-sulfonic acid (Wako) diluted in citrate buffer (0.1 M citrate buffer, pH 4.1) at RT for 20 min. The reaction was stopped with 0.1 M citric acid, and optical densities were measured at 415 nm using a precision microplate reader (Molecular Devises, Sunnyvale, CA). Two independent assays were performed in duplicate.

2.9. Statistical analysis

The growth inhibition assays were analyzed using a one-way ANOVA test to compare means. If the overall test was significant, Bonferroni's pairwise multiple comparison tests were used to